# CEBAF Program Advisory Committee Nine Proposal Cover Sheet

This proposal must be received by close of business on Thursday, December 1, 1994 at:

CEBAF
User Liaison Office, Mail Stop 12 B
12000 Jefferson Avenue
Newport News, VA 23606

## Proposal Title

Electron Scattering From A High-Momentum Nucleon In Deuterium

## Contact Person


**Name:** Dr. Sebastian E. Kuhn
**Institution:** Old Dominion University
**Address:** Department of Physics
**Address:** 1021 47th St.
**City, State ZIP/Country:** Norfolk, VA 23529
**Phone:** (804) 683 - 5804 **FAX:** (804) 683 - 5809
**E-Mail → Internet:** kuhn@cebaf.gov


**Experimental Hall:** B **Days Requested for Approval:** 16

**Hall B proposals only, list any experiments and days for concurrent running:**

NONE

**CEBAF Use Only**

Receipt Date: 12/14/94 PR 94-102

By: JP

# LAB RESOURCES REQUIREMENTS LIST

CEBAF Proposal No.: _____ Date: _____
(For CEBAF User Liaison Office use only.)

List below significant resources — both equipment and human — that you are requesting *from CEBAF* in support of mounting and executing the proposed experiment. Do not include items that will be routinely supplied to all running experiments, such as the base equipment for the hall and technical support for routine operation, installation, and maintenance.

***Major Installations*** *(either your equip. or new equip. requested from CEBAF)*

_____

_____

_____

_____

_____

_____

_____

_____

_____

New Support Structures: _____

_____

_____

***Data Acquisition/Reduction***

Computing Resources: _____

_____

_____

New Software: _____

_____

_____

***Major Equipment***

Magnets _____

_____

Power Supplies _____

_____

Targets _____

_____

Detectors _____

_____

Electronics _____

_____

Computer Hardware _____

_____

Other _____

_____

***Other***

_____

_____

_____

_____

_____

ONLY STANDARD EQUIPMENT AND SOFTWARE IS NEEDED

# HAZARD IDENTIFICATION CHECKLIST

CEBAF Proposal No.: _____ Date: _____
(For CEBAF User Liaison Office use only.)

Check all items for which there is an anticipated need.

**Cryogenics**
- ___ beamline magnets
- ✓ analysis magnets
- ___ target
  - type: _____
  - flow rate: _____
  - capacity: _____

**Electrical Equipment**
- ✓ cryo/electrical devices
- ___ capacitor banks
- ✓ high voltage
- ___ exposed equipment

**Radioactive/Hazardous Materials**
List any radioactive or hazadorous/ toxic materials planned for use:
- ✓

**Pressure Vessels**
- < 1 cm inside diameter
- ≈ 20 atm operating pressure
- Havar window material
- ___ window thickness

**Flammable Gas or Liquids**
- type: $D_2$
- flow rate: —
- capacity: ≈ 10 cm³

**Drift Chambers**
- type: Ar - Ethane
- flow rate: Standard
- capacity: _____

**Other Target Materials**
- ___ Beryllium (Be)
- ___ Lithium (Li)
- ___ Mercury (Hg)
- ___ Lead (Pb)
- ___ Tungsten (W)
- ___ Uranium (U)
- ___ Other (list below)

**Vacuum Vessels**
- ___ inside diameter
- ___ operating pressure
- ___ window material
- ___ window thickness

**Radioactive Sources**
- ___ permanent installation
- ___ temporary use
- type: _____
- strength: _____

**Large Mech. Structure/System**
- ___ lifting devices
- ___ motion controllers
- ___ scaffolding or
- ___ elevated platforms

**Lasers**
- type: _____
- wattage: _____
- class: _____

Installation:
- ___ permanent
- ___ temporary

Use:
- ___ calibration
- ___ alignment

**Hazardous Materials**
- ___ cyanide plating materials
- ___ scintillation oil (from)
- ___ PCBs
- ___ methane
- ___ TMAE
- ___ TEA
- ___ photographic developers
- ___ other (list below)

**General:**

Experiment Class:
- ✓ Base Equipment
- ___ Temp. Mod. to Base Equip.
- ___ Permanent Mod. to Base Equipment
- ___ Major New Apparatus

Other: _____

# ELECTRON SCATTERING FROM A HIGH–MOMENTUM NUCLEON IN DEUTERIUM

**A Proposal for an Experiment using the CEBAF Large Acceptance Spectrometer**

S.E. KUHN (Spokesperson), G.E. DODGE, C.E. HYDE-WRIGHT,
A. KLEIN, L. QIN, B.A. RAUE, L.B. WEINSTEIN, P.E. ULMER
*Old Dominion University, Norfolk, VA 23529*

K.A. GRIFFIOEN (Spokesperson), J.M. FINN
*The College of William and Mary, Williamsburg, VA 23187*

S. STEPANYAN, M. SARGSYAN, K. EGIYAN, R. DEMIRCHYAN, H. EGIYAN
*Yerevan Physics Institute, Yerevan, Armenia*

W. BROOKS
*CEBAF, Newport News, VA*

B. QUINN
*Carnegie Mellon University, Pittsburgh, PA*

and the CLAS Collaboration

**Abstract**

We propose to measure inelastically scattered electrons in coincidence with protons emitted backwards relative to the virtual photon direction in the reaction $d(e,e'p)X$. Using a 6 GeV electron beam and the CLAS detector, we can study this reaction for a large range of proton momenta ($0.25 - 0.6$ GeV/c) and electron kinematics ($Q^2 = 1 - 6$ GeV$^2$/c$^2$, $x = 0.2 - 1$).

In a simple spectator model, the electron scatters off a forward-moving neutron inside the deuteron and the detected backward-moving proton is an undisturbed spectator. Its measured momentum is equal and opposite to the momentum of the neutron before it was struck. By measuring the semi-inclusive cross section as a function of spectator momentum and direction, we can study the dependence on kinematics and off-shell behavior of the electron-nucleon cross section in the elastic, resonance, and deep inelastic region. At the same time we will gain information on the high-momentum structure of the deuteron wave function.

On the other hand, if the virtual photon couples to a quark in a 6-quark object, the spectator picture breaks down and a quite different dependence of the cross section on the kinematic variables ($x$, $Q^2$, and $\vec{p}_s$) will be observed. If such a 6-quark object exists as part of the deuteron wave function, it will be more easily detected in the kinematic region which favors short internucleon distances, i.e., at the high relative nucleon momenta observed by the proposed experiment.

We ask for 16 days of running on a deuterium target with an unpolarized 6 GeV beam in Hall B. The statistics collected in that time will be sufficient to study the dependence on all kinematic variables in appropriately small bin sizes. We note that the trigger requirements are not stringent and the running conditions are quite flexible, thus ensuring that a large body of data will be collected that can be analysed for many other purposes.

## 1. INTRODUCTION

One of the currently fascinating questions in nuclear physics is at what level does the quark-gluon picture supersede the nucleon-meson picture? Clearly, when the wave functions of two nucleons overlap significantly one can expect large changes in the internal structure of the nucleons. This may lead to a change in form factors and structure functions (depending on the off-shell mass, $m^*$, of the struck nucleon) or, in the extreme case, to a complete fusion of the two nucleons into a 6-quark object. The chance of a significant nucleon overlap occurring in nuclei is rather high. The probability of finding a nucleon inside a nucleus with internal momentum above the Fermi surface ($\geq$ 300MeV/c) is about 25% for heavy nuclei, and results primarily from 2-nucleon correlations[1]. Even in deuterium, approximately 3$-$4% of the momentum-space wave function lies above 300 MeV/c and possibly 2% lies above 400MeV/c. By designing experiments that are sensitive to short-range correlations in nuclei, we can amplify the effects of microscopic degrees of freedom. We wish to concentrate our efforts on the simplest nucleus, deuterium, for which the interpretation of the data is easiest and realistic calculations exist[1,2,3,4,5]. In this case, the two baryons making up the correlation ($np$, $\Delta\Delta$, etc.) have equal and opposite internal momenta. By detecting a backward-going baryon with high momentum, we can ensure that the reaction occurred on a tightly correlated pair and we can measure its internal momentum. We wish to investigate several aspects of the d(e,e'p)X reaction:

(a) Can we describe the scattering process in a spectator picture where the backward going nucleon is undisturbed by the reaction that occured on the correlated forward going nucleon? If the spectator picture is correct then we expect that the cross section will depend only on those variables that describe the free cross section, after a kinematical correction for the motion of the struck nucleon.

(b) What is the correct description of the deuteron wave function? Does one need light cone wave functions[1] or a fully relativistic description[3] ? One avenue to answer some of these questions would be to integrate the scattering cross section over large kinematic ranges of $x$ and $Q^2$ at fixed spectator momentum and then to study the dependence of the integrated cross section on the spectator momentum. The dependence on the direction of the spectator momentum, for example, is quite different for light cone dynamics and non-relativistic deuteron models.

(c) How are the nucleon form factors and structure functions modified for high-momentum nucleon-nucleon correlations? Within the spectator picture one could study off-shell elastic and transition form factors. One can compare resonance transition amplitudes to the free values to gain insight into possible deformations of nucleons inside tightly correlated pairs. Data in the deep inelastic region address several issues including interpretations of the EMC effect, techniques for extracting the neutron structure functions from measurements on the deuteron, and the existence of 6-quark or $\Delta\Delta$ configurations.

The experiment proposed here (inelastic electron scattering off deuterium with

coincident detection of a proton in the backward hemisphere relative to $\vec{q}$) has been discussed before in a letter of intent[6] and more recently at the Workshop on CEBAF at Higher Energies[7]. It can be naturally extended to heavier nuclei, such as $^3He$, $^4He$, $^{12}C$ and $^{56}Fe$, as described partially by the existing multi-hadron proposals for the CLAS detector[8]. Deuterium has originally been included in that proposal as a standard of comparison for experiments on complex nuclei. The unique perspective of the present proposal lies in the exclusive concentration on deuterium as the lightest nucleus and the emphasis on the highest available beam energies, enabling us to reach the Björkèn scaling region. We believe that the fundamental mechanism of kinematic rescaling and any possible modifications of elastic and inelastic structure functions, as well as possible non-nucleonic configurations of correlated nucleons inside nuclei, must first be studied well in the relatively simple A=2 system. The interpretation of measurements on heavier nuclei is much more complicated since final state interactions can influence the spectrum of spectators as well as produce additional backward-going nucleons which are difficult to separate experimentally from the spectator nucleons. Also, deuterium is the only nucleus where the center of mass of the correlated pair is guaranteed to be initially at rest in the laboratory frame.

A common proposal for observing short-range correlation effects is to look at inclusive electron scattering off deuterium in the kinematic region $x_{\rm Bj} > 1$. Since the free nucleon structure functions fall off rapidly as $x_{\rm Bj} \to 1$, the cross section will be sensitive to the high-momentum components of the deuteron wave function, where the scattering occurs on a fast-moving nucleon coming toward the virtual photon. The problem with the $x > 1$ measurements is that there is no way to determine the momentum of the struck nucleon and the data are averaged over a number of true $x$-values for a fixed $x_{\rm Bj}$. Not only does the tagged structure function method proposed here provide similar information to the $x > 1$ measurements, it actually provides this information in much richer detail!

## 2. THEORETICAL BACKGROUND

The (inclusive) cross section for scattering of an electron with initial four-momentum $e$ and final four-momentum $e'$ off a free nucleon is given by

$$\frac{d\sigma}{dxdQ^2} = \frac{4\pi\alpha_{\rm EM}^2}{Q^4}\left[y^2F_1(x,Q^2) + (1 - y - \frac{m^2y^2x^2}{Q^2})\frac{F_2(x,Q^2)}{x}\right] \qquad (1)$$

where $Q^2 \equiv -q^2 = -(e-e')^2 = \vec{q}^2 - \nu^2$ is the negative 4-momentum squared of the virtual photon, $x = Q^2/2p\cdot q$, $p$ and $m$ are the initial four-momentum and mass of the struck nucleon, respectively, and $y = p\cdot q/p\cdot e$. Finally, $\alpha_{\rm EM}$ is the fine-structure constant. For a nucleon at rest, $p\cdot q = m\nu$, and $x$ becomes $x = x_{\rm Bj} \equiv Q^2/2m\nu$ (Björkèn-$x$). In the spectator model of inelastic scattering, the virtual photon is absorbed on a nucleon (moving with momentum $\vec{p}$), while the other nucleon is a

spectator to the scattering (moving with momentum $\vec{p}_s = -\vec{p}$). If that second nucleon is truly a spectator, then it must be on-shell at the time of the scattering, with energy $E_s = \sqrt{m^2 + \vec{p}^2}$. Energy conservation requires that the other nucleon must be off-shell with energy $E^* = \sqrt{m^{*2} + \vec{p}^2}$, where $E_s + E^* = M_D \simeq 2m$. In this case $p \cdot q = E^*\nu - \vec{p} \cdot \vec{q}$. This can be rewritten as

$$p \cdot q = (2m - E_s)\nu - p_{||}q = m\nu(2 - [E_s + p_{||}(q/\nu)]/m). \quad (2)$$

In the limit $q/\nu \to 1$, the second term on the right becomes $(\sqrt{m^2 + \vec{p}_s^{\,2}} - p_{s||})/m \equiv \alpha$, and $x \approx x_{\rm Bj}/(2-\alpha)$. The light-cone fraction $\alpha$ of the momentum of the deuteron carried by the spectator nucleon is normalized to have values from 0 to 2 (two nucleons). The approximation $q/\nu = \sqrt{1 + Q^2/\nu^2} = \sqrt{1 + x_{\rm Bj}2m/\nu} \approx 1$ becomes valid to within 10% for the kinematics of this experiment.

If the spectator picture is correct, then the cross section for scattering from an off-shell nucleon will depend on the same Lorentz-invariant variables, $Q^2$, $x$, and $y$, as the on-shell cross section (Eq. 1), and on the invariant off-shell mass $m^*$. These are the only non-trivial Lorentz-invariants that one can build using the four-momenta $e$, $e'$, and $p$. On the other hand, if the observed backward proton was directly involved in the scattering process (due to Final State Interactions – FSI – or other two-nucleon effects), there are two additional invariants that can be constructed from the measured quantities $e$, $e'$, $p_s$, and $P_D$ (the initial four-momentum of the deuteron). One can choose the beam energy $E \equiv e^0$ and the energy transfer $\nu = e^0 - e'^0$ to represent these additional variables. In principle, the semi-inclusive cross section will depend on these quantities explicitly even if $m^{*2}$, $Q^2$, $x$, and $y$ are kept constant. By looking for such an explicit dependence on $E$ and $\nu$ we can assess the validity of the spectator picture (see next section).

If the spectator picture is validated (at least for certain kinematic regions), we can study several aspects of the electron-neutron cross section for off-shell neutrons. These will now be discussed in more detail.

### *2.1. Deep Inelastic Scattering*

The dominant effect in deep inelastic scattering is a rescaling of the variable $x \approx x_{\rm Bj}/(2-\alpha)$ from its value for a free nucleon at rest. This results in a kinematic shift of the deep-inelastic structure functions $F_1$ and $F_2$. This effect is most pronounced at high spectator momentum and large backward angles. In the most straightforward extension of the on-shell cross section (Eq. 1) this rescaling is the only change and we can write the semi-inclusive cross section (using light cone variables) as[1]

$$\frac{d\sigma_{\rm 2N}}{dx dQ^2 d\alpha d^2p_\perp} = \frac{4\pi\alpha^2_{\rm EM}}{Q^4}\left[y^2F_1(x,Q^2) + (1 - y - \frac{m^2y^2x^2}{Q^2})\frac{F_2(x,Q^2)}{x}\right]|\psi_{LC}(\alpha,p_\perp)|^2 \quad (3)$$

in which $\psi_{LC}$ is the momentum-space deuteron wave function expressed in terms of the light cone fraction $\alpha$ and the transverse momentum $p_\perp$. Using a non-relativistic

form of the deuteron wave function, this equation becomes

$$\frac{d\sigma_{2N}}{dxdQ^2d^3p} = \frac{4\pi\alpha^2_{EM}}{Q^4}\left[y^2F_1(x,Q^2) + (1-y-\frac{m^2y^2x^2}{Q^2})\frac{F_2(x,Q^2)}{x}\right]|\psi_{NR}(|\vec{p}|^2)|^2 \quad (4)$$

The connection between the light cone formulation, Eq. 3, and the non-relativistic counterpart, Eq. 4, can be seen from the relationship[1]

$$|\psi_{LC}(\alpha,p_\perp)|^2 d\alpha d^2p_\perp = |\psi_{NR}(|\vec{k}|^2)|^2 d^3k \quad (5)$$

where the "internal momentum" $\vec{k}$ is given by

$$\vec{p}_\perp = \vec{k}_\perp; \alpha = \frac{k_{||}}{\sqrt{m^2+\vec{k}^2}} + 1 \quad (6)$$

It can be inferred from Eq. 6 that the measured spectator momentum component $p_{||}$ along the q-vector is smaller than the internal momentum component $k_{||}$. This leads to a more rapid fall-off of the cross section in Eq. 3 with $p_{||}$ than in the non-relativistic picture of Eq. 4. Also, the light cone cross section becomes explicitly dependent on the direction of the spectator momentum (in addition to the rescaling of $x$ mentioned above). These different predictions will be tested by the proposed experiment.

At present, the existing experimental data are sparse and do not allow us to investigate in detail the structure of the cross section (Eq. 3 or 4) as a function of all kinematic variables. The Big European Bubble Chamber (BEBC) collaboration has studied deep inelastic neutrino scattering in coincidence with the emission of a single backward-going nucleon[9]. They calculate the average value of the observed Björken-$x$, $< x_{Bj} >$, for their total data set and the average observed Björken-$x$, $< x_{Bj} >_\alpha$, for several bins in the light cone fraction, $\alpha$, of the backward-going nucleons. Since $\alpha$ and the "true" scaling variable $x$ are uncorrelated, one expects a relation of the form

$$\frac{< x_{Bj} >_\alpha}{< x_{Bj} >} = 2 - \alpha. \quad (7)$$

The BEBC data taken for deuterium and for neon indeed show this correlation. Unfortunately, this is not conclusive proof for the validity of the spectator model. In fact, any object with baryon number $A = 2$ that fragments into a backward-going nucleon will produce a similar kinematic relationship[10]. Hence, for a better understanding of the light-cone structure of two close nucleons it is crucial to map out the tagged structure functions rather than to rely on gross averages. In heavier nuclei, particles in the backward direction coming from nucleon-nucleon correlations will be masked by nuclear re-interactions or cascading even for events that contain only a single backward-going nucleon. Recent preliminary results from E665 at Fermilab bear this out for Xenon[11]. On the other hand, most theoretical analyses[2,12] agree that FSI and direct hadronization do not contribute significantly in the kinematic region chosen for our experiment on deuterium.

Going beyond the most simple extrapolation from the free nucleon, one has to consider several additional effects: The structure functions for the off-shell nucleon could depend explicitely on $m^*$ and there could be more structure functions than in the on-shell case[5]. Several theoretical treatments have studied the change in the deep inelastic structure functions as a function of $m^*$ and/or changes in the nucleon radius[3,13,5,14]. These authors predict a reduction of the deep inelastic structure functions proportional to $m^*/m$, which reaches $1\% - 10\%$ (depending on $x$) even for the rather loosely bound neutron in deuterium ($m^*/m \approx 0.976$ on average). In our experiment, we can easily reach $m^*/m = 0.68$ (for $|\vec{p}_s| = 0.5$ GeV/c) which should yield reductions of at least 20%. This can be disentangled (at least partially) from the deuteron wave function $\psi(\alpha, p_\perp)$ by studying the $x$-, $y$- and $Q^2$-dependence of the cross section. For example, Frankfurt and Strikman[1] have proposed a simple model for off-shell effects in the light cone formalism which is based on the assumption that point-like configurations (PLC) of the nucleon are suppressed by a factor

$$\delta_D(|\vec{k}|) = \left[\frac{1}{1 + 2E_s/\Delta E_D}\right]^2 \tag{8}$$

if the nucleon is bound to another nucleon with relative momentum $\vec{k}$. Here, $E_s(\vec{k}) = \vec{k}^{\,2}/2m + \epsilon_D$ is the separation energy of a nucleon with momentum $\vec{k}$ and $\Delta E_D$ is the energy scale for nucleonic excitations in deuterium. The suppression of PLC leads to a linear decrease of the structure functions $F_1$ and $F_2$ from their free values at $x = 0.3$ to a value reduced by the factor $\delta_D(|\vec{k}|)$ at and above $x = 0.6$ (see Fig. 19). Quite a different picture emerges in a calculation based on the Sullivan model[3], where binding leads to an increase in the nucleon–plus–pion Fock state component over the free nucleon wave function. Here, the ratio $F_2{}^n(x, |\vec{p}_s|)/F_2{}^n(x)_{free}$ is *increased* for nearly all $x$ (by as much as 10% at $x = 0.2$) and falls off smoothly towards $x = 1$. Furthermore, the effect is not increasing monotonically with $|\vec{p}_s|$, but reverses at $|\vec{p}_s| > 0.5 GeV/c$. A mapping out of both $x$- and $|\vec{p}_s|$-dependence will enable us to distinguish between these two theoretical results.

### *2.2. The 6-quark model*

In contrast to the spectator picture, we can imagine the opposite extreme, for which the two nucleons are kneaded into a 6-quark (6q) object. Although no more than 5% of the deuteron wavefunction could be due to 6q states (deduced from overlap arguments), above 0.3 GeV/c relative nucleon momentum, a large fraction (even as much as $50 - 100\%$) of the wavefunction might be in a 6q configuration.

Several years ago, Lassila and Sukhatme[15] deduced estimates for the valence and sea quark distributions in an object with $N$ valence quarks using dimensional counting rules and available data on $N = 2$ and $N = 3$ systems. This is the starting point of our model for a 6-quark structure function. The valence distribution, assumed to have the same form for each quark flavor, is

$$V_N(x) = B_N x^{-1/2}(1 - x)^{b_N} \tag{9}$$

and the sea distribution is

$$O_N(x) = A_N x^{-1}(1-x)^{a_N}, \tag{10}$$

in which $x$ is the fraction of the N-quark object's momentum carried by the struck quark. The condition

$$\int_0^1 V_N(x)dx = 1 \tag{11}$$

insures that $V_N$ is normalized per valence quark. This integration can be performed using

$$\int_0^1 x^a(1-x)^b dx = \frac{\Gamma(a+1)\Gamma(b+1)}{\Gamma(a+b+2)} \tag{12}$$

in which the standard $\Gamma$-function obeys the relation $\Gamma(a+1) = a\Gamma(a)$. Therefore,

$$B_N = \frac{\Gamma(b_N + \frac{3}{2})}{\Gamma(\frac{1}{2})\Gamma(b_N+1)} \tag{13}$$

The fraction of the momentum carried by the valence quarks is simply

$$z_V = N\int_0^1 xV_N(x)dx = \frac{N}{2b_N+3} \tag{14}$$

Momentum conservation demands that $z_V + z_O + z_g = 1$, in which $z_O$ is the fractional momentum carried by the sea quarks and $z_g$ is that carried by the glue. If we define $\xi = z_0/z_g$, which by some estimates is about $\frac{1}{5}$ and independent of N, then

$$z_O = \frac{2b_N+3-N}{2b_N+3}\frac{\xi}{1+\xi} \tag{15}$$

Fits to the available pion and proton data yield

$$b_N = 2N-3 \tag{16}$$

and

$$a_N = N+6, \tag{17}$$

with an uncertainty of about $\pm 1$. In the parton model, the structure function $F_2(x) = \sum_i e_i^2 x q_i(x)$, in which $q_i(x)$ is the quark distribution function and $e_i$ is the charge of the $i$-th quark flavor. We will assume that the strange quarks have half the weight of u and d quarks in the sea. Therefore, $\bar{u} = \bar{d} = \frac{1}{5}O_N(x)$ and $\bar{s} = \frac{1}{10}O_N(x)$. The valence quark content of the proton is uud, of the neutron is udd and of the deuteron is uuuddd. Hence,

$$F_2^{\text{sea}}(x) = \frac{11}{45}xO_N(x) \tag{18}$$

for all particles. However,

$$F_2^{\text{valence}}(x) = \eta x V_N(x) \tag{19}$$

| $N$ | $a_N$ | $b_N$ | $A_N$ | $B_N$ |
|---|---|---|---|---|
| 2 | 8 | 1 | 0.90 | 0.75 |
| 3 | 9 | 3 | 1.11 | 2.19 |
| 6 | 12 | 9 | 1.55 | 1.47 |

Table 1: Constants for the N-quark model

in which $\eta = 1$, $2/3$ and $5/3$ for proton, neutron, and 6-quark object, respectively. Table 1 shows the calculated values of the constants required for pion ($N = 2$), proton ($N = 3$) and 6-quark object ($N = 6$).

Conventionally, nuclear structure functions are normalized per nucleon and $x$ runs from 0 to $A$. Hence, for the 6-quark case, we must divide $F_2$ by two and evaluate it at $x/2$, in which the measured $x$ can run from 0 to 2. Since we plan to observe a backward-going proton, the electron will strike the neutron. Hence, within the schematic model above, we can write

$$r(x) \equiv \frac{F_2^{6q}}{F_2^n} = \frac{1.22\sqrt{x/2}(1-x/2)^9 + 0.19(1-x/2)^{12}}{1.46\sqrt{x}(1-x)^3 + 0.27(1-x)^9} \tag{20}$$

which is valid for $x < 1$ only. A more realistic estimate of $F_2^{6q}$ follows by taking $r(x)$ times the NMC parametrization of $F_2^n = 2F_2^d - F_2^p$. This assumes that the $Q^2$ evolution and the higher twist is identical for scattering from 6-quark objects and neutrons.

After a 6-quark object is struck by a high-energy electron, one quark will be scattered and the remaining five will fragment into observable particles. Again, since we detect a proton, we are interested in the fragmentation function $D_p^{5q}(z, p_T)$, in which $z$ is the fraction of the 5-quark momentum carried by the observed proton, and $p_T$ is that proton's transverse momentum. Following the model of Carlson, Lassila and Sukhatme[16], we can take $D(z) \propto z^n(1-z)^3$. On average, the protons produced should have $3/5$ of the available 5-quark momentum, since it is created with 3 of these 5 quarks. Therefore,

$$< z >= \frac{3}{5} = \frac{\int_0^1 z^{n+1}(1-z)^3 dz}{\int_0^1 z^n(1-z)^3 dz} = \frac{n+1}{n+5} \tag{21}$$

Hence, we take $n = 5$. Estimates from existing data show that the $p_T$ distribution is nearly gaussian in $p_T^2$. The fully normalized fragmentation function (integral = 1) is

$$D_p^{6q}(z, p_T) = \frac{1008}{\sqrt{\pi}(0.34\text{GeV})} z^5(1-z)^3 e^{-p_T^2/(0.34\text{GeV})^2}. \tag{22}$$

The full 6-quark cross section then becomes

$$\frac{d\sigma}{dx_{Bj}dQ^2d\alpha dp_T} = \frac{4\pi\alpha_{EM}^2}{Q^4}\left[1-y-\frac{Q^2}{4E^2}+\frac{y^2+Q^2/E^2}{2(1+R(x_{Bj},Q^2))}\right]\cdot \frac{F_2^{6q}(x_{Bj},Q^2)}{x_{Bj}}\left(\frac{1}{2-x_{Bj}}\right)D_p^{5q}(\frac{\alpha}{2-x_{Bj}},p_T) \quad (23)$$

in which the extra factor of $1/(2-x_{Bj})$ comes from the transformation from $z$ to $\alpha$. Here, $R(x_{Bj},Q^2)=(\vec{q}^2/\nu^2)(F_2/2xF_1)-1$ is the ratio of longitudinal to transverse virtual photon cross section.

In order to compare this cross section with the data, Carlson and Lassila[10] have proposed to determine the ratio

$$R=\frac{\sigma_{\rm measured}}{KF_2(\frac{x_{Bj}}{2-\alpha})}, \quad (24)$$

where $K$ is the factor in the first line of Eq. 23. In the spectator model (without off-shell effects) $R$ becomes $R=(2-\alpha)|\psi(\alpha,p_\perp)|^2$ (the factor $(2-\alpha)$ arises from the definition of $\sigma_{\rm measured}$ in terms of $x_{Bj}$ instead of $x$). Obviously, the ratio $R$ would be constant for fixed $\alpha$ and $p_\perp$ in that case. However, if one scatters from a 6q object, $R$ will vary with $x$. In this case,

$$R=\frac{F_2^{(6)}(x_{Bj})D_{\rm N/5q}(z,p_\perp)}{(2-x_{Bj})(2-\alpha)F_2(\frac{x_{Bj}}{2-\alpha})}. \quad (25)$$

The $x$-dependence of Eq. 25 is quite different from that predicted by the off-shell model discussed above, as can be seen from Fig. 19.

The true story in deuterium probably lies somewhere between the spectator and 6q extremes. However, these two models serve to provide a scale for the magnitude of the possible effects we can observe. If $R$ is indeed flat with $x$ one can perhaps set constraints on the 6q content of the deuteron. If $R$ is not flat with $x$ it will provide the first quantitative evidence for modification of the structure functions (beyond simple kinematics) when two nucleons get close to each other.

### *2.3. Resonance Region*

In the kinematic region where the final state of the struck neutron in the reaction $d(e,e'p)X$ is either a nucleon resonance or a free neutron ("elastic" scattering), one can again observe several aspects of the cross section on a bound nucleon.

The major expected effect is the kinematic shift of the resonance and elastic peaks due to the motion of the struck nucleon. Therefore it is interesting to investigate the dependence of the scattered electron spectra on the momentum and angle of the backward proton. The appropriate variable to use in this case is not $x$ but the invariant mass squared $W^2=m^{*2}+2p\cdot q-Q^2$. The kinematic position of the well

known resonance structures[17] is governed by the relativistically correct invariant mass squared, $W^2$, as defined above, instead of the corresponding quantity for a nucleon at rest, $m^2+2m\nu-Q^2$. This leads to the following approximate relationship between the electron energy loss, $\nu_{res}(\alpha)$, needed to excite a given resonance with mass $W_{res}$ and the corresponding energy loss, $\nu_0$, on a free nucleon:

$$\nu_{res}(\alpha) \approx \frac{W_{res}^2 - m^{*2} + Q^2}{2m(2-\alpha)} = \frac{m^2 - m^{*2}}{2m(2-\alpha)} + \frac{\nu_0}{(2-\alpha)} \tag{26}$$

Equation 26 demonstrates that the resonance peaks are shifted by a fixed offset for given spectator momentum $|\vec{p}_s|$ (off-shell mass $m^*$)† and are "stretched out" by a rescaling factor $1/(2-\alpha)$. It follows that with increasing momentum of the backward proton, the distance between the quasielastic peak and the resonance peaks will increase, and the resonance structure will be smeared out. To visualize this, we show in Fig. 1 the scattered electron energy spectra for several spectator momenta. The figure shows that in the case of $|\vec{p}_s| > 0.3$ GeV/c the electron spectrum is almost flat and does not reveal any pronounced "bumps". However, the same spectra represented in terms of $W$ (Fig. 2) reproduce the familiar resonance structure. Note that this prediction is based on more than just a simple kinematical relationship. Other possible reaction mechanisms (such as rescattering etc.), which are not sensitive to high internal momenta of nucleons in the deuteron and do not lead to factorization, will not necessarily produce the same resonance structure (with the same relative strength, shape, and $Q^2$ dependence of each peak) as in the case of electron scattering on the free nucleon. In the extreme case of a complete breakdown of the spectator picture, one no longer sees individual resonance peaks at the correct values of $W$. Instead one might find direct evidence of $\Delta\Delta$ [18] or 6-quark configurations in the deuteron or even dibaryon resonances. Further information on the reaction mechanism can be obtained simultaneously with the semi-inclusive data by observing the final state of the struck neutron.

After we have assessed the validity of the spectator model, we can again look for off-shell effects in the excitation cross section for each resonance peak. Such effects might be indicative of possible changes in the bound nucleon radius or "shape". The parameter controlling the amount by which the struck neutron is off shell is $m^2 - m^{*2} \equiv m^2 - (p_d^\mu - p_s^\mu)^2$ and is fixed by the absolute value of the momentum of the backward proton. To separate off-shell effects from the kinematic shift discussed above one has to keep the electron variables $\nu$ and $\vec{q}$, as well as the angle $\theta_{pq} = \arccos(\hat{p}_s \cdot \hat{q})$, constant. Since the uncertainty in the deuteron wave function makes a direct comparison of different $p_s$ ambiguous, it is advantageous to look for off-shell modifications of the ratio between longitudinal and transverse structure functions instead. This is equivalent to varying the remaining variable, $y$. There

†It is interesting to note that the one-to-one relationship between $x$ and $W$ at fixed $Q^2$ is no longer valid here since the off-shell mass $m^*$ enters explicitly. This can be considered as another $m^*$-dependent effect on the structure functions.

are essentially two ways to accomplish this[19]: One can either keep $\nu$,$\vec{q}$, and $\vec{p}_s$ fixed and study the cross section for different beam energies (using the data from existing proposals at 4 GeV [8,18]) or one can make use of the out-of-plane capability of CLAS. Specifically, by comparing cross sections for different azimuthal angles, $\phi_{pq}$, between the $(\vec{p}\,\vec{q})$ and $(\vec{q}\,\vec{e})$ planes at given values of $\nu$, $\vec{q}$, $p_s$, one can look at the $y$-dependence at fixed beam energy.

There exist several different theoretical approaches to treat the scattering of high energy electrons off deeply bound nucleons (see e.g. Refs.[20,21,1,22,23,19]). They predict similar cross sections for low internal nucleon momenta but disagree strongly for higher momenta. In Fig. 3 we present, for illustration, the predictions of different calculations for the $y$-dependence of the cross section in the case of quasielastic scattering ($W_{res} = m$). For each model, we plot the ratio $R = \frac{\sigma(\phi_{pq}=180°)}{\sigma(\phi_{pq}=90°)}$, normalized to the corresponding ratio calculated within the on-shell approximation.

In the special case $W^2 = m^2$ one studies the reaction $d(e,e'p)n$. The underlying physics (deuteron structure[24], FSI and meson exchange currents, and deformation of the bound nucleon, see above) is being investigated extensively both at CEBAF[25] and other laboratories. The unique perspective that our experiment could bring to bear is the fact that we look at quasielastic scattering off the neutron (not the proton, as is usually the case), and that we will have complete out-of-plane coverage which does not exist elsewhere for these high $Q^2$.

In practice, the information extracted might be contaminated to some extent by Final State Interactions (FSI) which are estimated to be rather large[26,27,28] if the production of fast backward protons is dominated by the contribution of short range configurations. The experimental measure of FSI in the considered reaction can be defined as follows:

$$\kappa = \frac{\sigma^{exp}}{\sigma^{PWIA}} \tag{27}$$

where $\sigma^{exp}$ is the measured $d(e,e'p)n$ cross section and $\sigma^{PWIA}$ is the cross section calculated within the framework of the Plane Wave Impulse Approximation.

In Fig. 4, predictions for the dependence of $\kappa$ on the proton angle, $\theta_{pq}$, are presented for different values of the proton momentum. The calculation was done within the Glauber model which accounts properly for relativistic effects specific to high energy processes[28]. These calculations predict that $\kappa$ should have a peak near $\theta_{pq} \approx 60°$ at proton momenta $|\vec{p}_s| \geq 400$ MeV/c (corresponding to $\alpha \approx 1$).

The proposed experiment will check the predicted angular dependence of $\kappa$ and, therefore, verify the necessity of the relativistic Glauber approximation. In Fig. 5 the angular dependence of $\kappa$ is compared to the prediction of a nonrelativistic Glauber approximation[27]. It is seen that a considerable difference in the position of the maxima of $\kappa$ is predicted in these different approximations. The origin of this difference is that in a relativistic treatment of $pn$ rescattering the FSI will not change the $\alpha$ of the detected proton (see e.g. Refs.[1,28]) while the nonrelativistic treatment requires the conservation of the longitudinal component of the proton momentum.

## 3. EXPERIMENTAL DETAILS

The aim of the proposed experiment is to collect a large body of data that can be directly compared to the various theoretical approaches mentioned in the previous section. These models predict different behavior of the cross section $\frac{d\sigma_{2N}}{dxdQ^2d^3p}$ as a function of *all* kinematic variables, requiring us to cover as much of the accessible kinematic phase space as possible. Therefore, the present experiment is uniquely suited for the CLAS detector with its large acceptance (including out-of-plane detection of the backward proton). Using a beam energy of 6 GeV, we will be able to collect data simultaneously over a large range in $x$ ($x = 0.2 - 1.0$), $W$ (up to $W \approx 3$ GeV), $Q^2$ ($1.0 \leq Q^2 \leq 6.0$ (GeV/c)$^2$), $\vec{p}_s$ ($0.25 \leq p_s \leq 0.6$ GeV/c), and $y$. In addition, using CLAS will allow us to detect (some part of) the final state hadrons coming from the struck nucleon as well as the backwards emitted proton.

Our requirements for the running conditions of CLAS are rather loose. We can run with normal B-field direction (inbending electrons) and field strength or with reversed or reduced B-field (leading to a somewhat larger acceptance at lower $Q^2$ and larger backward angles, see below). Our trigger requirement is one electron and one additional charged track, although this could be relaxed even further if it turns out to be beneficial for other experiments. For our count rate estimates we assume a standard (unpolarized) deuteron target and standard luminosity $L = 10^{34}/s/cm^2$. Under these assumptions, 16 days of ideal running will be sufficient (but also necessary) to collect enough statistics to make significant distinctions between several models, as shown in the next section. The total number of events collected will be in excess of $3 \times 10^6$. Figs. 6–7 show a breakdown of this expected data sample as a function of spectator momentum $p_s$.

### *3.1. Acceptance*

The acceptance of CLAS was determined under the following assumptions: Beam energy 6 GeV, scattered electrons detected above 0.6 GeV energy and out to 45°, backward protons detected above 0.25 GeV/c momentum and at an angle relative to the direction of $\vec{q}$ of more than 90°. We used the Monte Carlo program FASTMC[29] together with a model event generator that produced LUND-type event files. These same event files were also used as input for a more realistic simulation of the CLAS detector based on GEANT[30] and for SDA[31] to cross-check the results obtained with FASTMC. Figure 8 shows a typical event as simulated by GEANT. The model event generator was based on Eq. 4 and used the free nucleon structure functions as input. In the deep inelastic region we used the SLAC parametrization[32] of the structure functions $F_2$ and $R$, rescaled to the kinematically correct value of $x$. In the resonance region, the Brasse parametrization[33] was used, again rescaled to the proper $W$. Since this parametrization is for protons only, we multiplied the resulting structure functions with a factor $[G_{Mn}/G_{Mp}]^2$ to approximate the neutron structure functions. The 2N final state was described with the free neutron form factors $G_{Mn}$ (Dipole form) and $G_{En}$ (Galster parametrization). Cross checks with

different models[24] were made, and the agreement was found to be within the model uncertainties.

Figure 9 shows the overall acceptance of CLAS for events with different backward proton momenta $p_s$. After taking both proton and electron acceptance into account, one gets an average acceptance of about 50% for the events of interest. The acceptance increases towards high proton momentum and can be explained readily in terms of the geometric "shadow" of the coils. There is also a "hard" cut-off at small electron angles (corresponding to $Q^2 \leq 1$ (GeV/c)$^2$ and at large proton angles ($\theta_{pq} > 150°$, see Fig. 10). Reversing the polarity of the CLAS magnetic field pushes these boundaries out by some small amount, but it is not clear that this advantage outweighs the problem of higher singles rates (at low $Q^2$) and less-than-optimal response of the Čerenkov counters.

Obviously, the limits of acceptance in the different physical quantities $Q^2$, $x$, $W$, $\alpha$, $\vec{p}_s$, etc. are strongly correlated (both by kinematics and by detector coverage). Figures 10–12 illustrate this for several combinations of variables at a fixed $Q^2$-bin of $2.0 \pm 0.5$ (GeV/c)$^2$. For instance, one can read off Fig. 11 that we can reach the deep inelastic region ($W \geq 2.0$ GeeV) for nearly all proton momenta below 0.6 GeV/c. Figure 12 shows that even for the rather large light-cone fraction $\alpha = 1.3$ we can still cover some range in $x$ (this range increases if we include different $Q^2$-bins).

For the analysis of the proposed experiment it will be important to understand the acceptance of CLAS at the few-percent (2–3%) level. This will be achieved using both extensive Monte-Carlo simulation, results from data at 4 GeV, and our own data on two-body break-up of the deuteron which is kinematically overdetermined.

### *9.2. Resolution*

The required resolution of all kinematic variables is not very stringent in this experiment. We need to know the momentum of the proton to within 2% and its direction to within 5°. Figures 13–14 show the results of a SDA-simulation of these resolutions, which stay within the given bounds. A more detailed simulation of multiple scattering of the protons in the target and the target walls gave a result consistent with those bounds, as well.

The electron variables can be measured with very good precision. The expected error in $Q^2$ (about 2.5%) is much smaller than needed (except possibly in the case of the two-body final state where we will have to average the theoretical cross section with the resolution function of CLAS for a more accurate comparison). The most relevant parameter is the resolution in the missing mass $W$ since it determines whether we can resolve the different resonance states and the "elastic" peak. The precision with which one can measure $W$ depends on both the electron and the proton resolution, since the proton momentum enters the formula for $W$. The simulation gave a Gaussian width of only 20 MeV for $W_{measured} - W_{true}$ (see Fig. 15), again well within our requirements.

| Event type | events | total generated events | cross section | count rate |
|---|---|---|---|---|
| $Q^2 > 1$ e, no p | 24564 | 50000 | 0.12 $\mu$b | 590/s |
| $Q^2 < 1$ no e, all p | 4368 | 50000 | 72 $\mu$b | 63000/s |
| $Q^2 < 1$ no e, backward p | 170 | 50000 | 72 $\mu$b | 2400/s |

Table 2: Accidentals rates from CELEG

### *3.3. Background*

The dominant source of possible background events are accidental coincidences between electrons and uncorrelated proton tracks. We have also studied secondary interactions of knocked-out protons within the target walls etc. and found this contribution negligible. Misidentification of the backward particle is also not a problem since, at the low momenta of interest, both time-of-flight and energy loss measurements can readily distinguish protons from pions and other hadrons. We also ascertained that the pion rate is not much larger than the proton rate in the back hemisphere.

Since the present experiment is essentially a double-arm coincidence experiment between an electron and a proton, we must be convinced that at a luminosity of $10^{34}/\text{cm}^2/\text{s}$ accidental coincidences do not overwhelm the signal. Estimates of these rates have been made using the program CELEG, which simulates elastic scattering, resonance excitation, and deep-inelastic scattering with special attention to the hadrons produced. CELEG, when run for the deuteron, generates backward-going protons from the spectator picture as well as products from resonance decay.

Many backward-going protons may be produced in a quasi-elastic scattering reaction at low $Q^2$ in which the electron disappears at small angles, beyond the acceptance of CLAS. If another electron is detected simultaneously, the scattering is misidentified by the random proton. Because we are interested in events with $Q^2 > 1$, and the primary source of backward protons comes from $Q^2 < 1$, we have generated two sets of CELEG data. The first consists of events with $Q^2 > 1$ for which the electron is detected but no backward proton is observed. The second contains events with $Q^2 < 1$ in which a single backward proton is observed, but the electron is missing. These data are then passed through the fast Monte Carlo simulation of the CLAS detector.

Fig. 16 shows the acceptance in proton momentum and laboratory angle for protons with no accompanying electrons. Proton momenta can reach 2-3 GeV/c, but only for forward angles. The proton momentum for angles greater than 90° is bounded below by the detector acceptance at about 250 MeV/c. In this case the backward protons come overwhelmingly from quasi-elastic scattering. The proton momentum distribution falls rapidly from 0.25 GeV/c to 0.5 GeV/c, in keeping with the momentum-space wavefunction for the deuteron.

Table 2 summarizes the rates and cross sections for the simulation. In each case, 50000 events were generated by CELEG. The cross section specified in the table is

the total cross section for all electron-scattering events that are accepted by CLAS. The number of events that satisify the specified criteria, as well as the detector acceptance, are listed in column 2. The ratio of this number to the total, times the cross section, times a luminosity of $10^{34}/\mathrm{cm}^2/\mathrm{s}$ gives the rates in the last column.

Estimates of the fraction of accidental events is given by the formula

$$\frac{\text{accidentals}}{\text{trues}} = \frac{R_{\text{no p}} R_{\text{no e}} \Delta\tau}{R_{\text{true}}} \tag{28}$$

in which the $R$'s are rates and $\Delta\tau$ is the resolving time of the experiment. From the spectator model Monte Carlo simulation, $R_{\text{true}} = 2/\text{s}$. A conservative estimate for the resolving time is $\Delta\tau = 1$ ns. Since we are interested only in events with a backward-going proton, only the first and third rows in the table contribute to the numerator. The accidentals to trues ratio, then, is $2400 \times 590 \times 1\text{ns} \,/\, 2 = 7 \times 10^{-4}$. Accidental coincidences can therefore be ignored.

## 4. EXPECTED RESULTS

In this section, we demonstrate the sensitivity of the proposed experiment to several aspects of the theoretical models described in section 2. Expected error bars are based on the requested beam time and quality as spelled out in the previous section.

### *4.1. Tests of the Spectator Model*

As outlined in section 2, the spectator model cross section (Eq. 3) should not depend explicitly on the beam energy, $E$, nor the electron energy loss, $\nu$, if the invariant variables $Q^2$, $x$ or $W^2$, $y$, and $m^*$ are kept constant (by varying the spectator direction and electron scattering angle simultaneously with $E$ or $\nu$). At a fixed beam energy of 6 GeV, we can test this by comparing the number of counts (corrected for acceptance) in two bins of $\nu$ which correspond to the same bin in $Q^2$, $x$, $y$ and $p_s$. For instance, for the 2N final state ($W^2 = m^2$), we can choose a bin of $Q^2 = 1.5 - 2.5$ GeV$^2$/c$^2$, $p_s = 0.275 - 0.325$ GeV/c, and $y = 0.2 - 0.23$, where we will have full acceptance for $\nu = 1.3 - 1.55$ GeV. We will be able to compare the number of counts in the first and second half of this range in $\nu$ to 4% accuracy.

To test the dependence on $E$, we can use the data that will be collected during an already approved experiment at 4 GeV [18]. For instance, for $W^2 = m^2$, $Q^2 = 1.5-2.5$ GeV$^2$/c$^2$, $p_s = 0.525-0.6$ GeV/c, and $y = 0.325-0.425$, we will be able to compare data at 4 GeV and 6 GeV to 3% accuracy. The sensitivity of these methods (and the bin sizes) can be even increased if we use a simple parametrization of the cross section in $y$ (based on Eq. 3) instead of a fixed bin.

### *4.2. Light-cone vs. Non-Relativistic Wave Function*

One characteristic of the light-cone description of the semi-inclusive cross section

(Eq. 3) is the explicit dependence on the angle $\theta_{pq}$ between spectator momentum and the virtual photon direction. While the overall cross section is always reduced relative to the non-relativistic expression Eq. 4, this suppression is most pronounced at large $\theta_{pq}$. Figure 17 demonstrates this point: Even at moderate recoil momenta ($p_s = 0.25-0.3$ GeV/c), the light cone cross section is lower than the non-relativistic one by a factor $\approx 0.85$ in near perpendicular kinematics ($\theta_{pq} = 90° - 110°$), while the reduction factor is $\approx 0.62$ at more backward angles ($\theta_{pq} = 130° - 150°$). As can be seen from Fig. 17, the statistical error bars will clearly be small enough to observe this kinematic behaviour. The reduction is even more dramatic at higher spectator momenta ($\approx 0.5$ at $p_s > 0.4$), making a significant measurement possible in spite of somewhat larger error bars.

### *4.3. Off-shell Effects*

We used the model of Frankfurt and Strikman (Eq. 8) to get an estimate of the quality and magnitude of off-shell effects that we could expect. We chose a somewhat larger value for the parameter $\Delta E_D$ than usual[1], namely $\Delta E_D = 1.0$ GeV. This value is motivated by the fact that delta-excitations in deuterium can only occur on both nucleons simultaneously. Also, this rather large value leads to an *average* off-shell effect in deuterium corresponding to a 2% reduction at medium $x$ (see Fig. 18). This is the lower bound on most models mentioned in section 2. This model leads to a rather modest "EMC-effect" in deuterium, as can be seen from Fig. 18. On the other hand, even with this rather conservative value of $\Delta E_D$, there are quite dramatic off-shell effects at high recoil momentum, as can be seen in Fig. 19. While the absolute value of the off-shell reduction of the cross section can be masked by the uncertainty in the deuteron wave function $|\psi(\alpha, p_\perp)|^2$, the dependence on $x$ for different spectator momenta, $p_s$, is rather dramatic and can be easily detected with the expected statistical uncertainty. Shown in Fig. 19 is also the result of a recent calculation by Umnikov and collaborators[3] that predicts a rather different off-shell behavior.

### *4.4. 6-quark configurations*

In Fig. 19, we also show the prediction of the model for a six-quark configuration as discussed in the theory section. While the absolute normalization of this curve is uncertain to some degree (due to our lack of knowledge of the deuteron wave function), the dependence on $x$ is strikingly different than that predicted by the off-shell models. This behavior should be discernible even if only some fraction of the cross section comes from 6-quark objects.

### *4.5. Resonance region*

Figure 2 shows the expected statistics for several different spectator momenta over the whole resonance region. We will be able to determine the shape of the

cross section in that region with high precision (a few percent) and small bin size. Both the kinematic shift and any strong off-shell effects will be readily apparent.

## 5. SUMMARY AND REQUEST

We request beam time equivalent to 16 days at 100% efficiency of 6 GeV beam on a deuterium target at luminosity $10^{34}$ in the CLAS detector in Hall B. We require full functionality of all forward EGN and Čerenkov detectors, the TOF scintillators and all three regions of drift chambers. No additional detectors or other modifications are needed. The experiment can be done as soon as a 6 GeV beam is available in CLAS.

The data collected will allow us to study the validity of several theoretical models of electron scattering from a bound nucleon and of the structure of the deuteron in terms of nucleon and quark degrees of freedom. We will be able to clearly distinguish between different descriptions of the deuteron wave function (non-relativistic, light-cone, fully relativistic), of off-shell effects, and of 6-quark components in deuterium.

## References


1. L.L. Frankfurt and M.I. Strikman, *Phys. Rep.* **76**, (1981) 215; *Phys. Rep.* **160**, (1988) 235; *Nucl. Phys.* **A497**, (1989) 155c.
2. G.D. Bosveld, A.E. Dieperink and A.G. Tenner, *Phys. Rev. C* **49** (1994) 2379.
3. A.Yu. Umnikov, L.P. Kaptari, K.Yu. Kazakov and F.C. Khanna, preprint **Alberta Thy 21-94**, (1994) and nucl-th/9407006, and preprint **Alberta Thy 38-94**, (1994); A.Yu. Umnikov, private communication.
4. C. Ciofi degli Atti and S. Simula, *Phys. Lett. B* **319**, (1993) 23.
5. W. Melnitchouk, A.W. Schreiber, A.W. Thomas, *Phys. Rev. D* **49**, (1994) 1183.
6. S.E. Kuhn and K.A. Griffioen, CEBAF Letter of Intent (1991).
7. S.E. Kuhn and K.A. Griffioen, in *Workshop on CEBAF at Higher Energies* (N. Isgur and P. Stoler, editors), (1994) 347.
8. K. Egiyan et al., *CEBAF proposal* **PR-89-036** (1989).
9. Matsinos, *et al.*, Z. Phys. C **44**, (1989) 79.
10. C.E. Carlson and K.E. Lassila, *William and Mary Report* **WM-94-101** (1994).
11. K.A. Griffioen, E665 Collaboration, private communication (1994).
12. C. Ciofi degli Atti and S. Simula, preprint **INFN-ISS 94/8**, (1994) and nucl-th/9409017.
13. S.A. Kulagin, G. Piller, W. Weise, *Phys. Rev. C* **50**, (1994) 1154.
14. S.A. Gurvitz and A.S. Rinat, TRIUMF preprint **TR-PR-93-77**, (1993) and nucl-th/9312019
15. K.E. Lassila and U.P. Sukhatme, Phys. Lett. **B209** (1988) 343.
16. C.E. Carlson, K.E. Lassila and U.P. Sukhatme, Phys. Lett. **B263** (1991) 277.
17. S. Rock, et al., *Phys. Rev. Lett.* **49** 1139 (1982).
18. B. Quinn et al., *CEBAF proposal* **PR-93-043**, (1993).
19. K.Sh. Egiyan, M.M. Sargsyan, CEBAF preprint **PR 93-001**, (1993).
20. J.W. Bos and J.H. Koch, preprint hep-ph/9409292, (1994).
21. G. Kälbermann, L.L. Frankfurt and J.M. Eisenberg, preprint hep-ph/9402344
22. T. de Forest Jr., *Nucl. Phys.* **A329** 232 (1983).
23. J. Mougey, *Nucl. Phys.* **A262** 461 (1976).
24. J.W. van Orden,CEBAF preprint **CEBAF-TH-94-20**, (1994).
25. P.E. Ulmer et al., *CEBAF proposal* **PR-94-004**, (1993).
26. L. L. Frankfurt, E. Piasetsky, M. M. Sargsyan and M. I. Strikman, NUCL/TH-9405003 May 1994, *Phys. Rev. C*, in press.
27. A. Bianconi, S. Jeschonnek, N.N. Nikolaev, B.G. Zakharov, preprint **KFA-IKP(Th)-1994-34**, (1994) and nucl-th/9409014
28. L. L. Frankfurt, W. R. Greenberg, G. A. Miller, M. M. Sargsyan and M. I. Strikman DOE/ER/40427-28-N94.
29. Fast Monte Carlo Program for the CLAS Detector, E.S. Smith, CLAS-

NOTE-90-003, (1990).
30. GEANT Simulation Program for CLAS, M. Guidal, CLAS-NOTE-93-013, (1993).
31. B. Niczyporuk, Computer Program "SDA" (unpublished).
32. L.W. Whitlow, SLAC-Report-357 (1990).
33. F.W. Brasse et al., Nucl. Phys. **B110**, (1976) 413.
*Z. Phys.* **A335** 431 (1990).

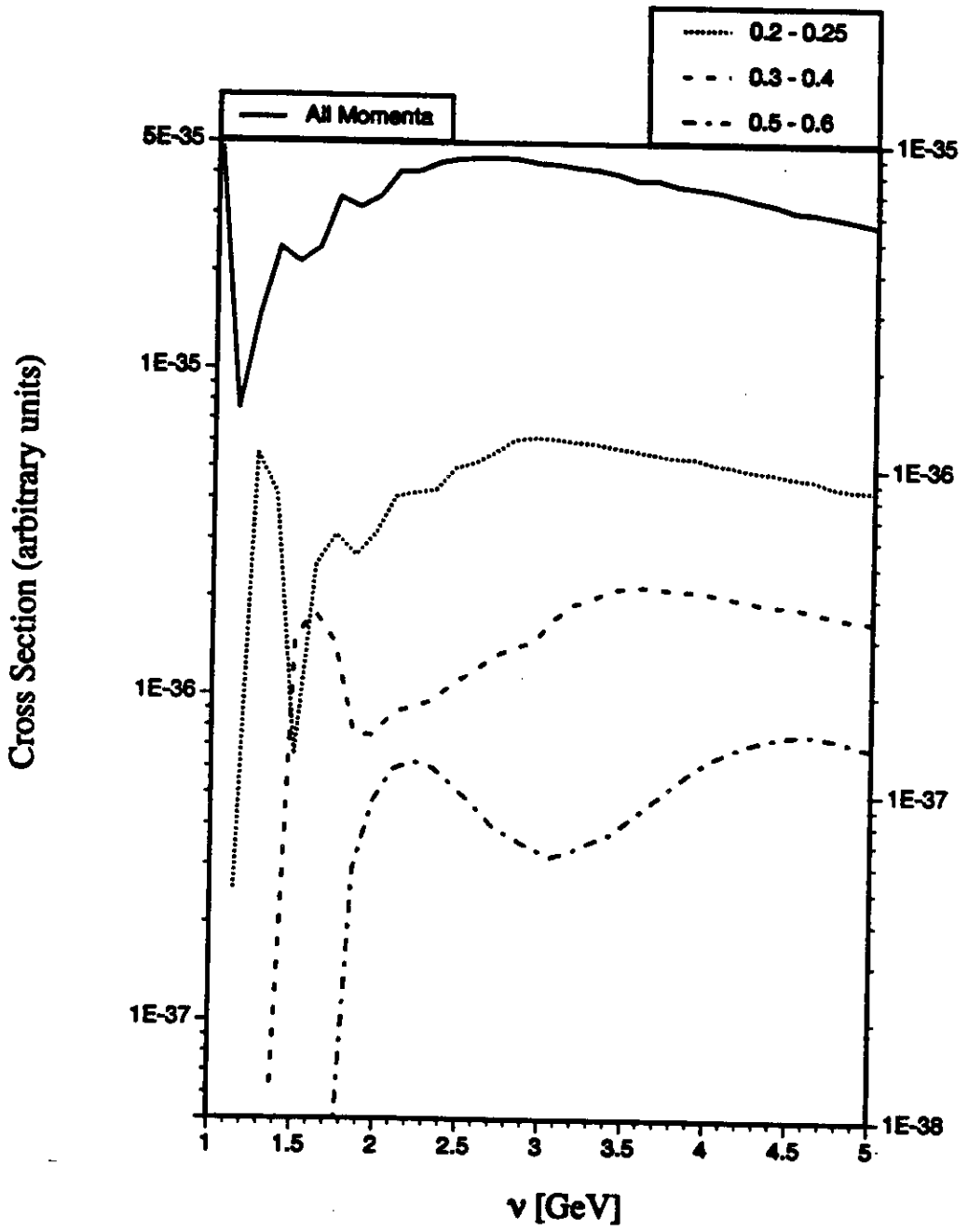


Fig. 1. Electron energy loss spectra in the spectator model for several spectator momenta and $Q^2 = 2$ (GeV/c)$^2$. The energy loss $\nu$ of the electron is calculated for the reaction d(e,e'p)X where the proton is emitted at $100° - 120°$ relative to $\vec{q}$, with momenta in the range $0.2 - 0.25$ GeV/c (dotted line), $0.3 - 0.4$ GeV/c (dashed line), and $0.5 - 0.6$ GeV/c (dot-dashed line). The solid line is averaged over all proton momenta in the same angular range. The resonance structure shows up clearly at low spectator momenta but is washed out due to the kinematic shift at $p_s \geq 0.3$ GeV/c.

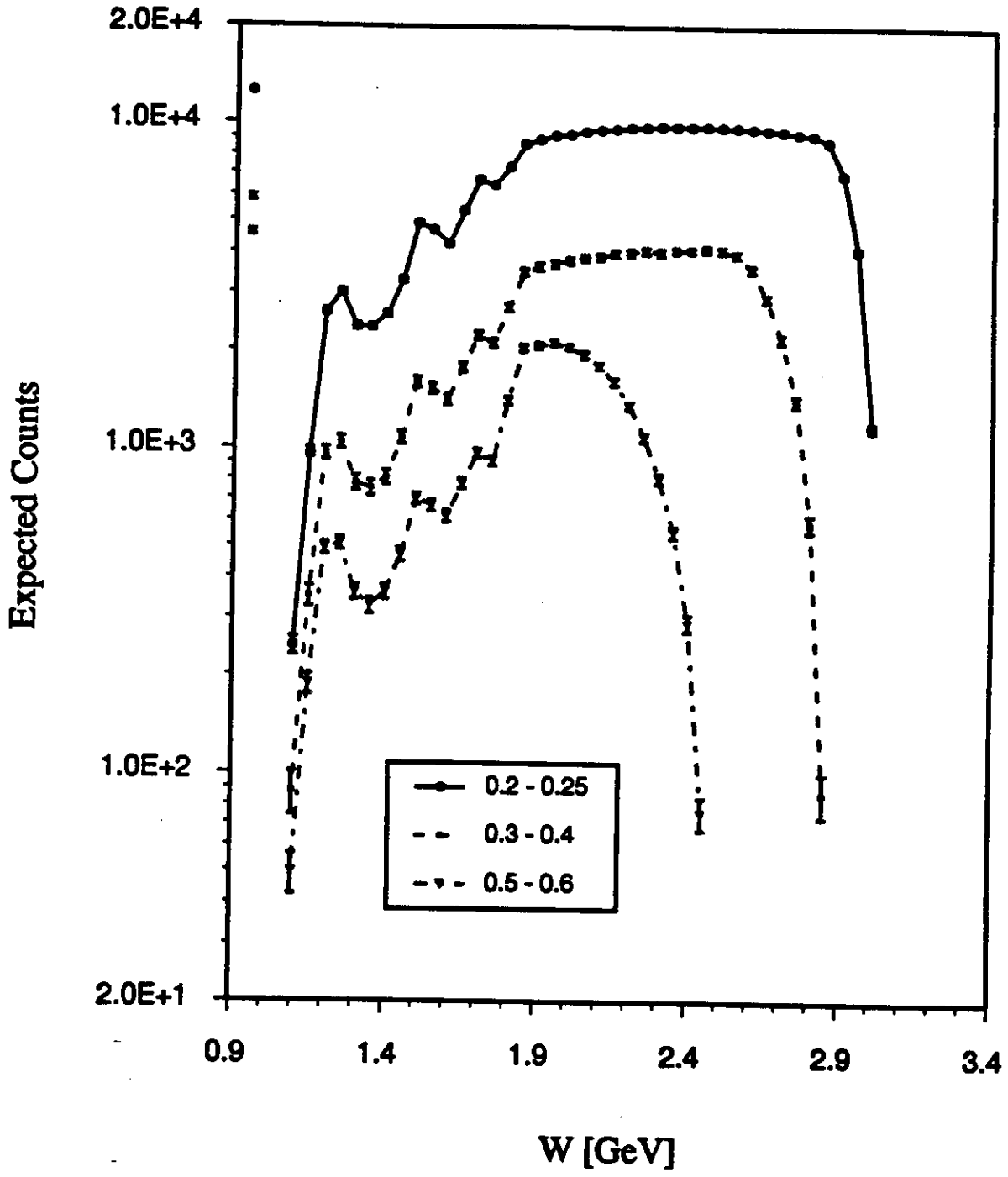


Fig. 2. Same spectra as in Fig. 1, rebinned in the invariant mass $W$ of the unobserved struck nucleon. The resonance peaks and the elastic peak appear clearly for all spectator momenta. The error bars indicate the statistical accuracy expected for the proposed experiment.

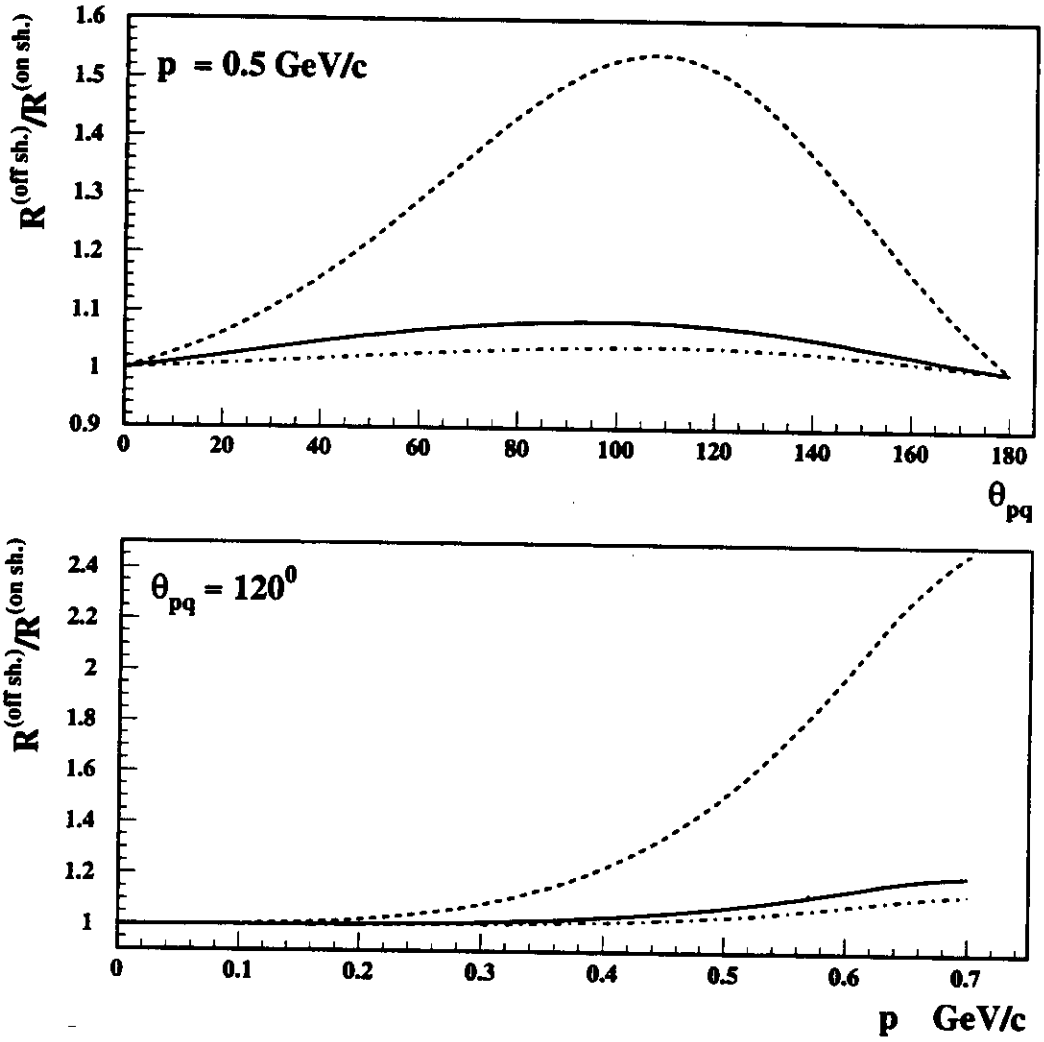


Fig. 3. Angular (upper panel) and momentum (lower panel) dependence of the ratio $\frac{R^{off}}{R^{on}}$ for the two-nucleon final state, where $R = \frac{\sigma_{eN}(\phi=180^0)}{\sigma_{eN}(\phi=90^0)}$ ($Q^2 = 1\ (GeV/c)^2$ and $E_e = 6\ GeV$). The solid line comes from an off-shell calculation of $\sigma_{eN}$ in the light-cone formalism[1,16]. The dashed line is the result of a calculation using the effective energy formalism according to Ref.[17] and the dash-dotted line is based on the effective mass formalism according to Ref.[18].

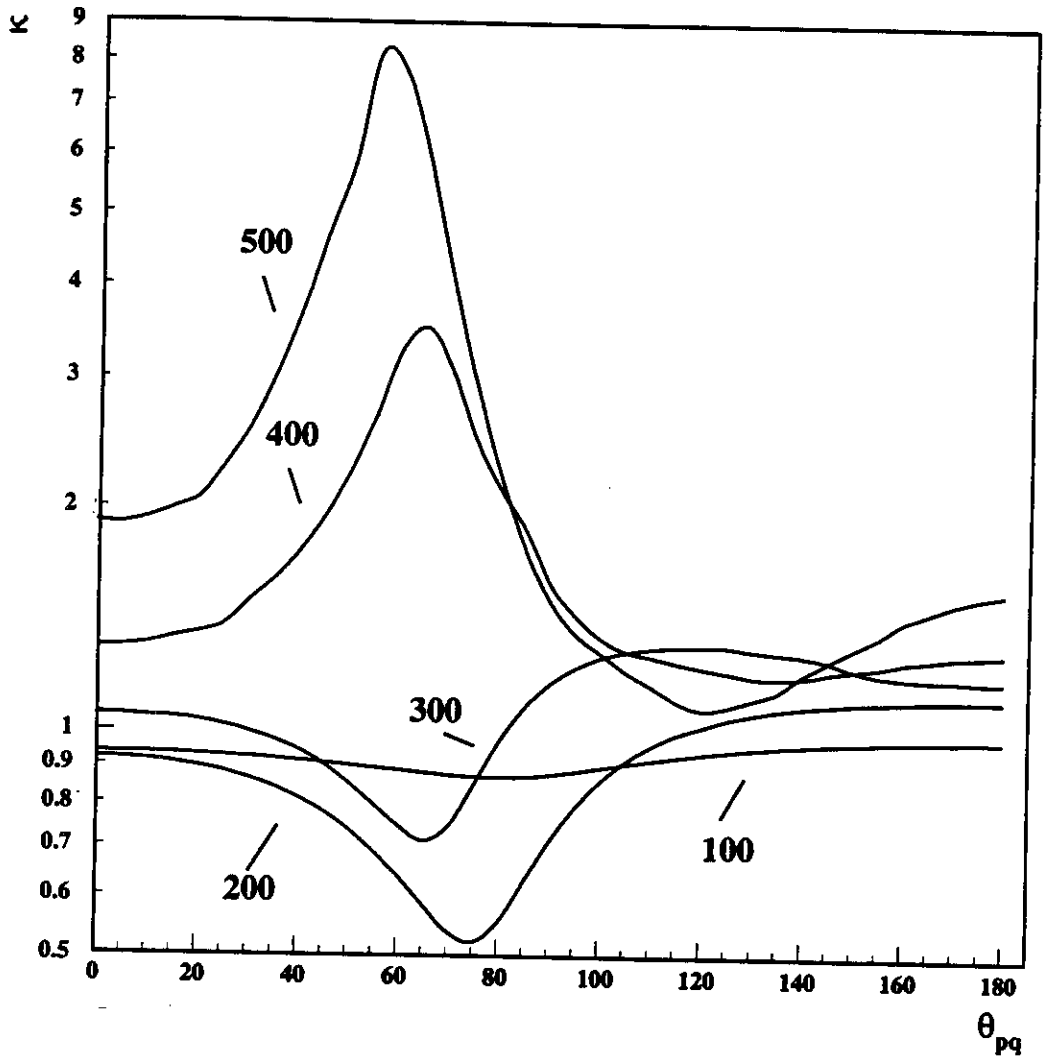


Fig. 4. Proton angular dependence of $\kappa = \frac{\sigma^{FSI}}{\sigma^{PWIA}}$, at $Q^2 = 1\ (GeV/c)^2$ and $E_e = 6\ GeV$ for the two-nucleon final state. The labels 500, 400, 300, 200, and 100 indicate the momentum of the spectator proton in MeV/c. The calculation was done with the Glauber approximation with relativistic modifications[34].

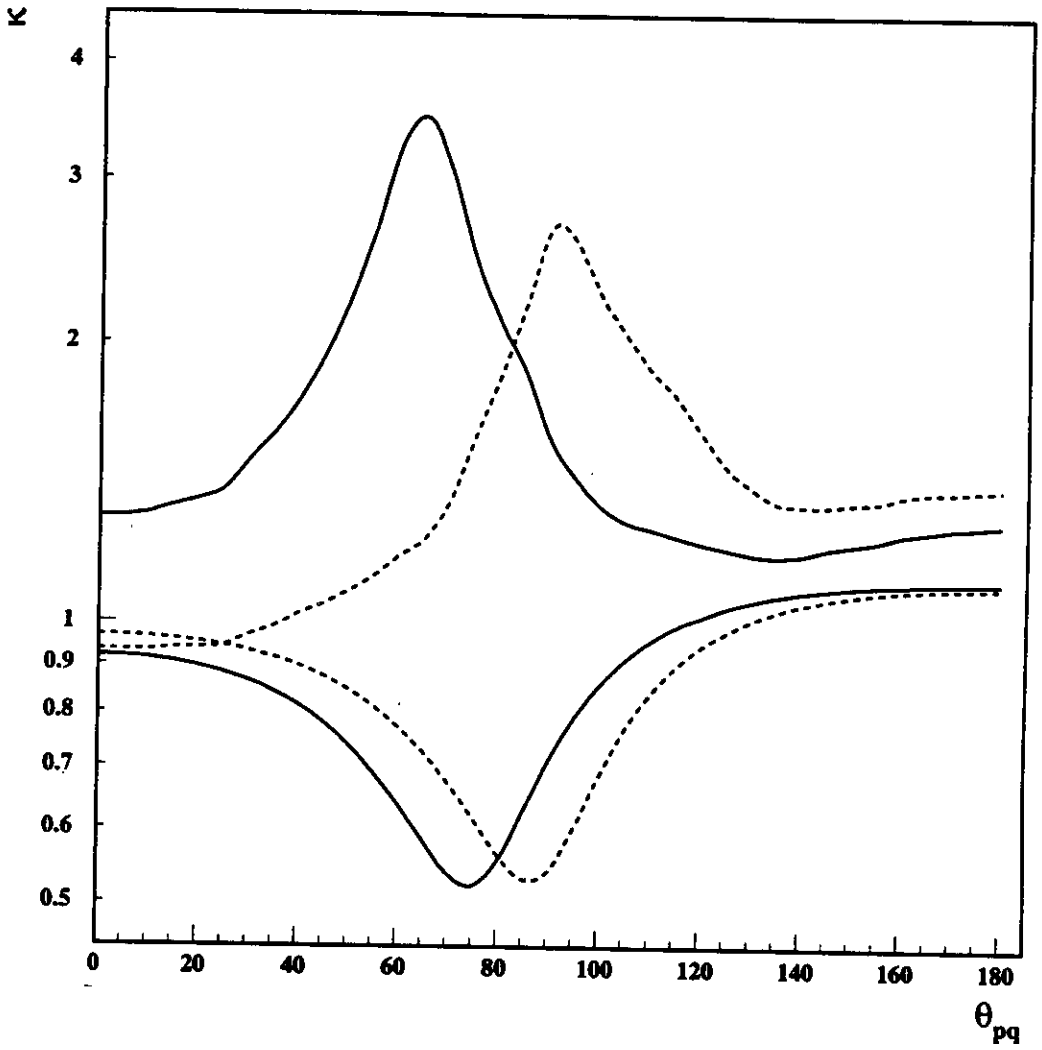


Fig. 5. Angular dependence of $\kappa$ for two different models of FSI. The upper (lower) solid line is the same as in the previous figure for $p = 400\ (200)\ MeV/c$. The dashed lines show the corresponding results from a calculation within the nonrelativistic Glauber approximation[13].

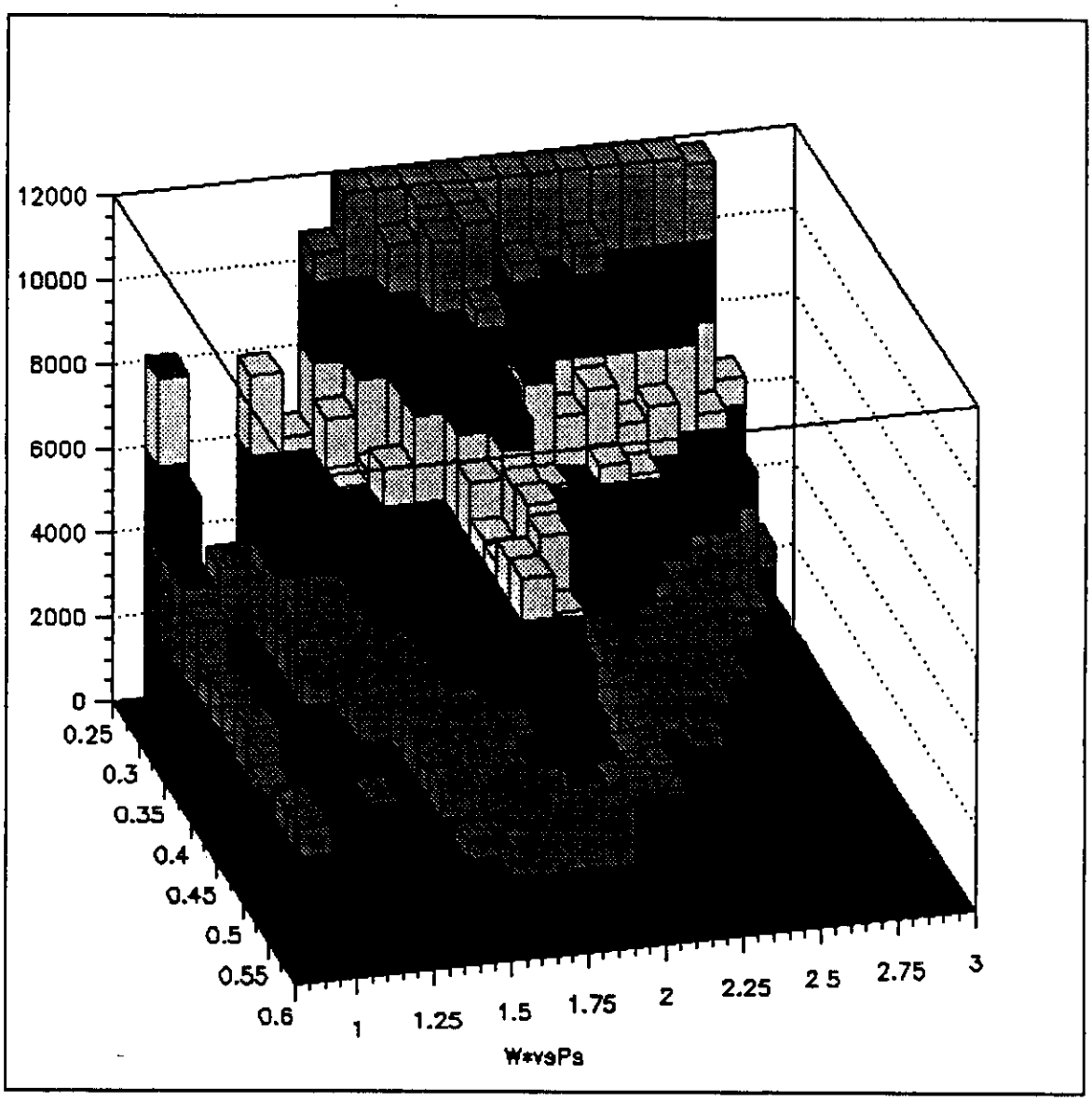


Fig. 6. Expected number of counts in each bin of $\Delta W = 0.1$ GeV and $\Delta p_s = 0.025$ GeV/c. This estimate is based on 16 days of running at full luminosity with a 6 GeV electron beam. The acceptance of CLAS at normal field polarity and full field strength is folded in. Only events in the $Q^2$-range $Q^2 = 1.5 - 2.5$ are included. All proton momenta are in the backward hemisphere relative to the q-vector.

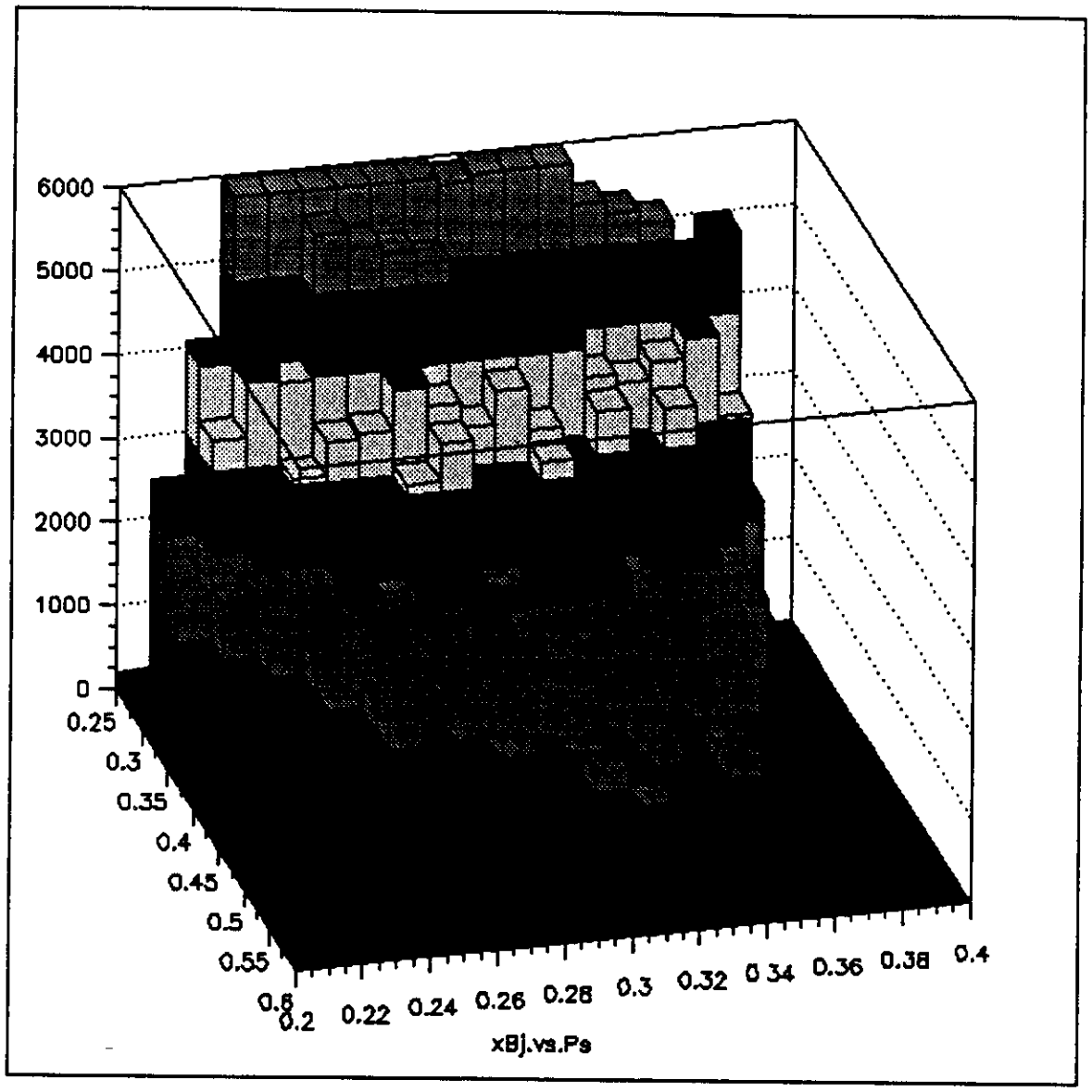


Fig. 7. Expected number of counts for each bin of $\Delta x = 0.02$ and $\Delta p_s = 0.025$ GeV/c for the same assumptions as in the previous figure.

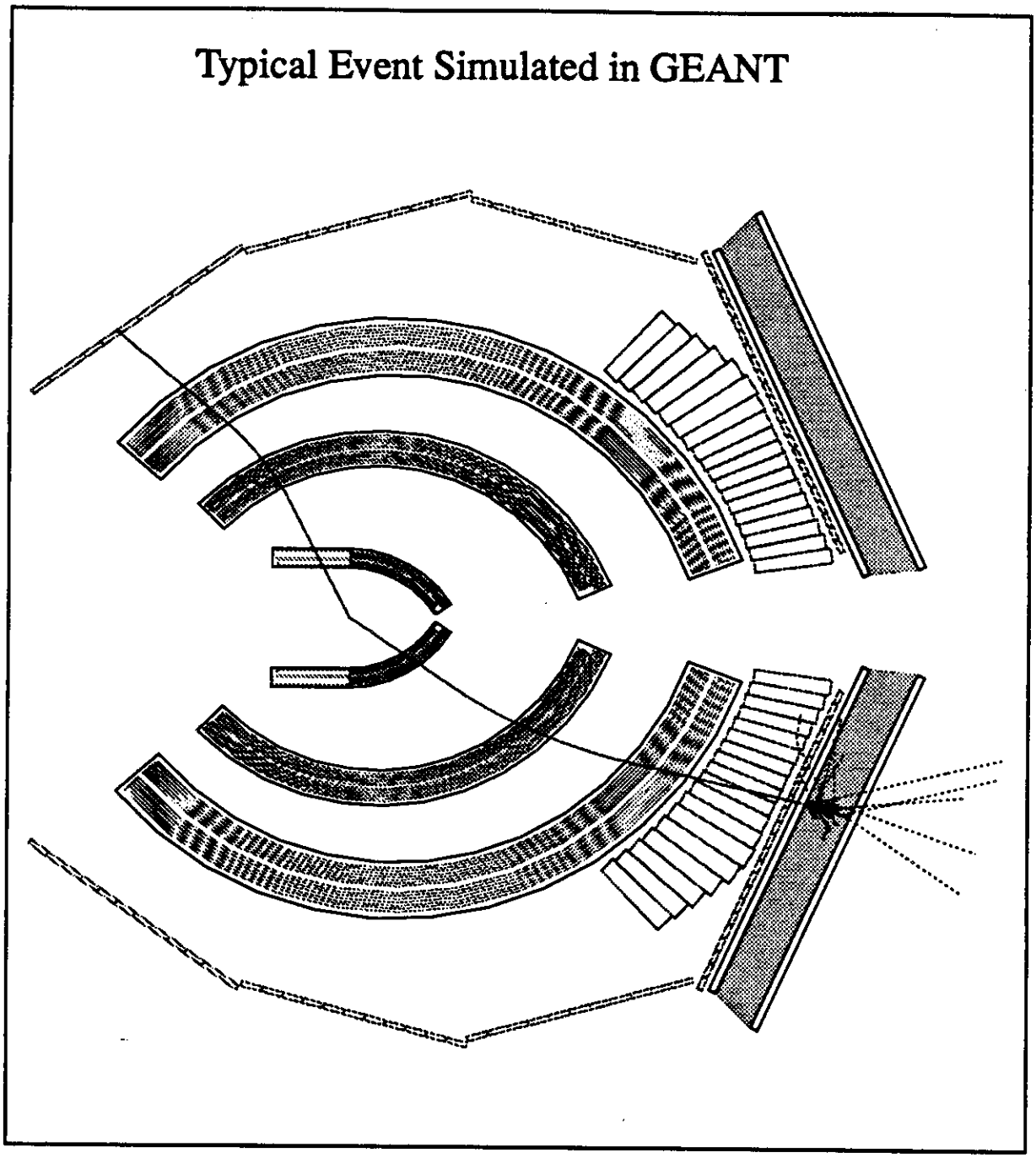


Fig. 8. Typical d(e,ep)X event as simulated with GEANT. The electron is going forward in the lower half of the spectrometer and the proton is going backward in the upper half. One can see that the proton is detected in all three drift chamber regions and the TOF counter.

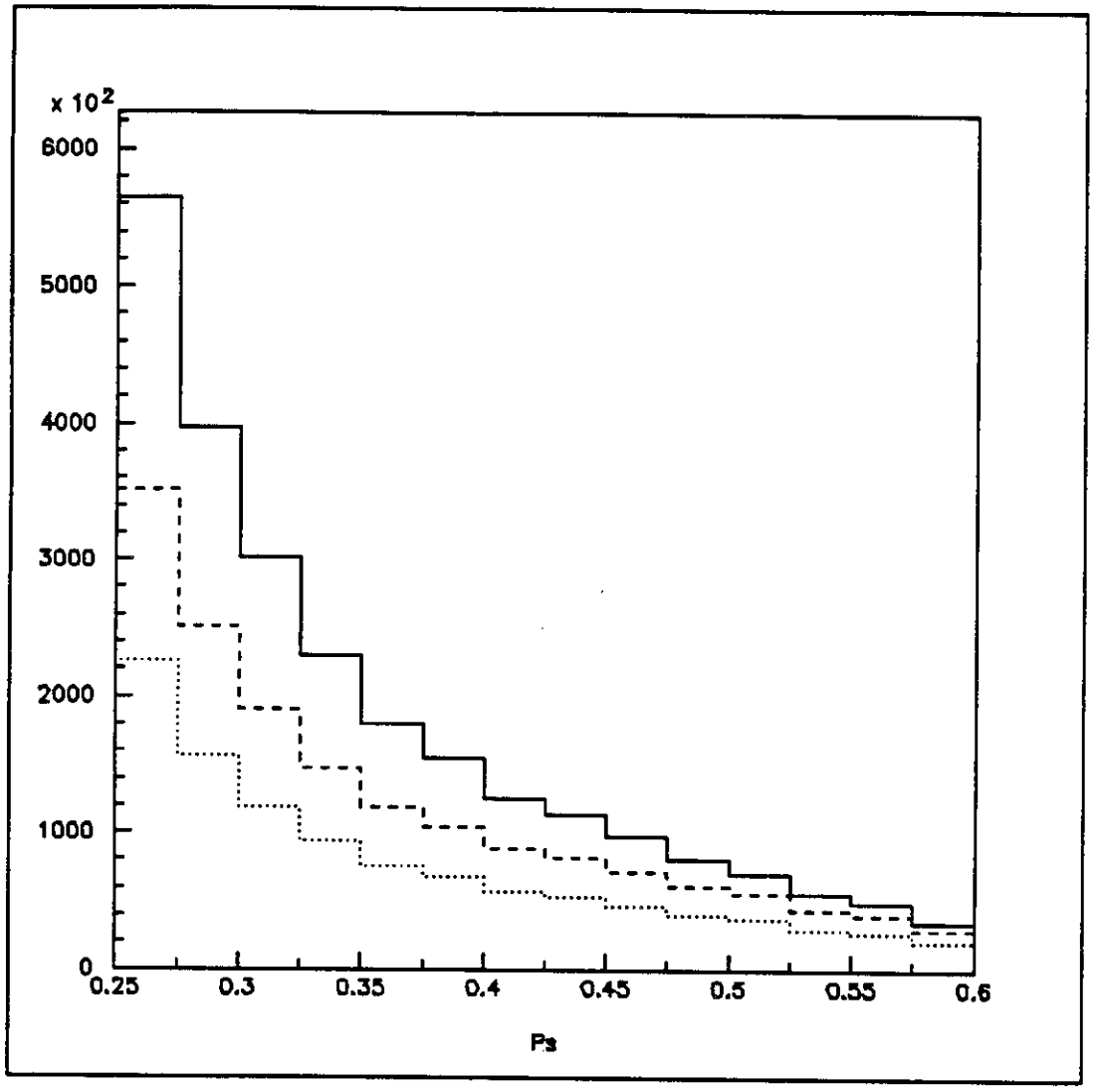


Fig. 9. Spectrum of spectator momenta to be observed in this experiment for the same assumptions as in Fig. 6. The solid line shows the distribution of events from the Monte Carlo event generator. The dashed line shows the number of events where the proton is within the CLAS acceptance. The dotted line includes the requirement that both proton and electron are detected in CLAS. Note the overall scale factor of 100!

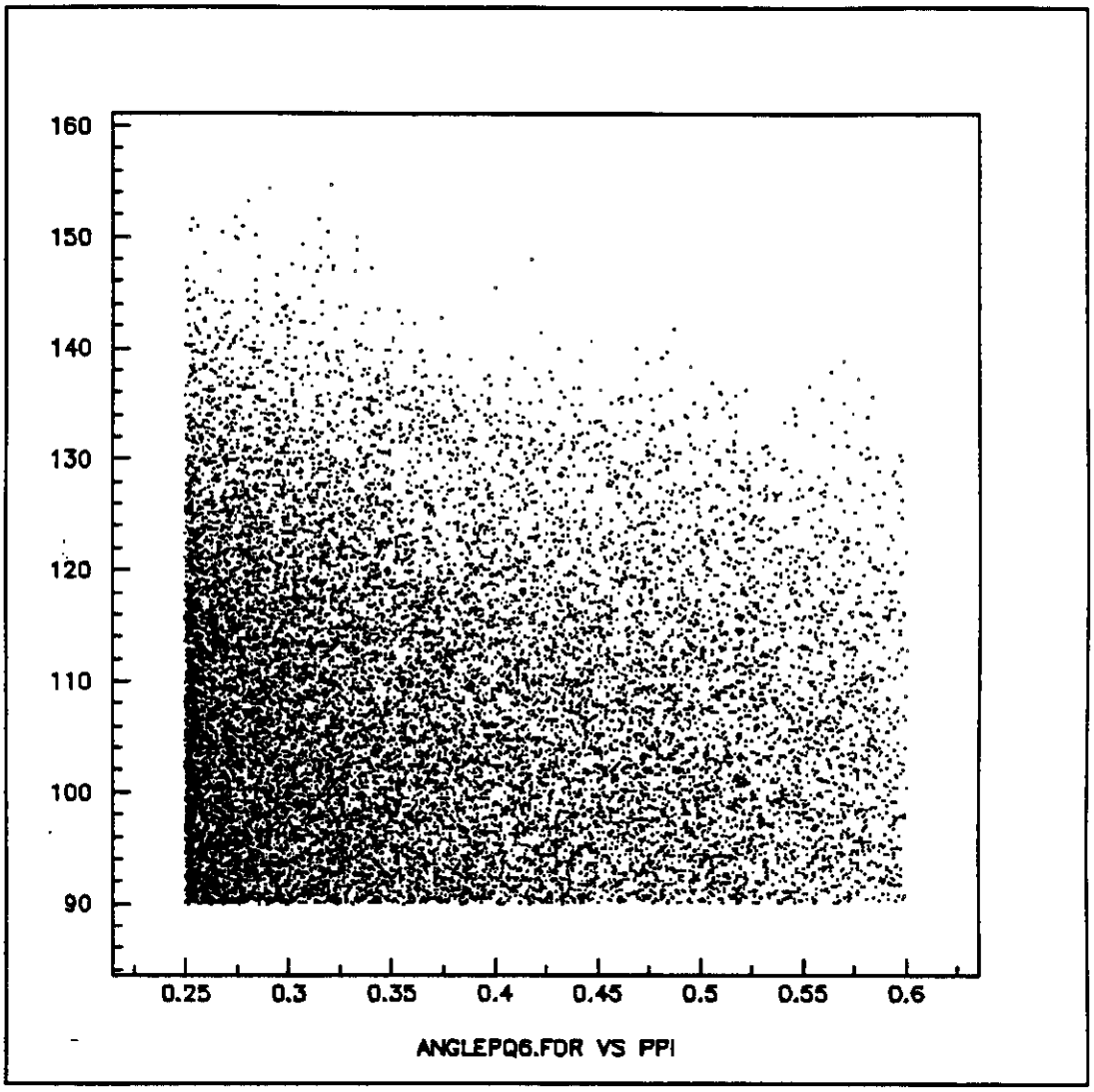


Fig. 10. Acceptance of CLAS for events with different proton momenta (horizontal axis) and angles $\theta_{pq}$ (vertical axis). Same assumptions as in Fig. 6.

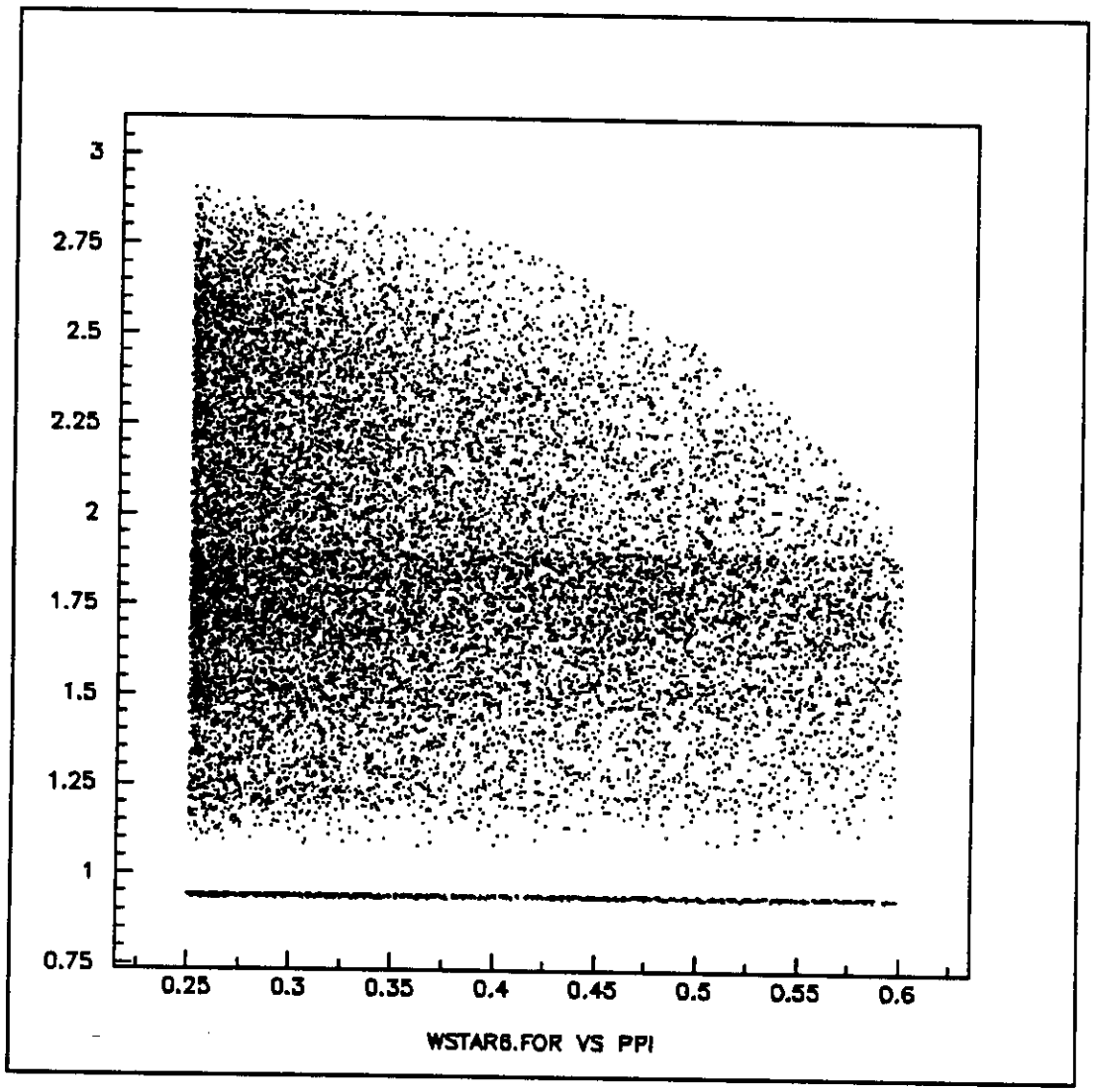


Fig. 11. Acceptance of CLAS for events with different proton momenta (horizontal axis) and invariant mass $W$ of the unobserved final state (vertical axis). Same assumptions as in Fig. 6.

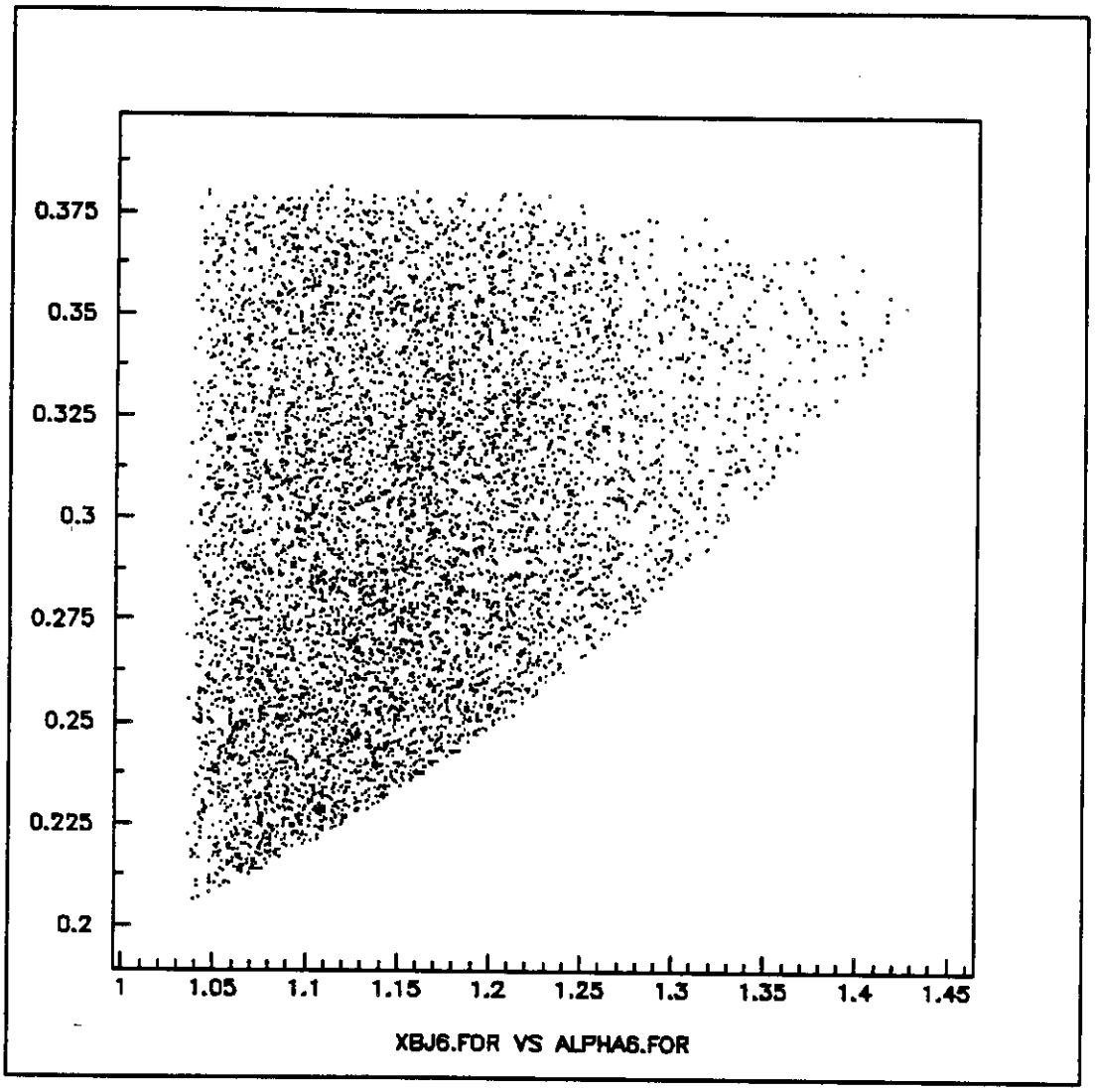


Fig. 12. Accessible range for $x$ (vertical axis) vs. light cone fraction $\alpha$ (horizontal axis). Same assumptions as in Fig. 6.

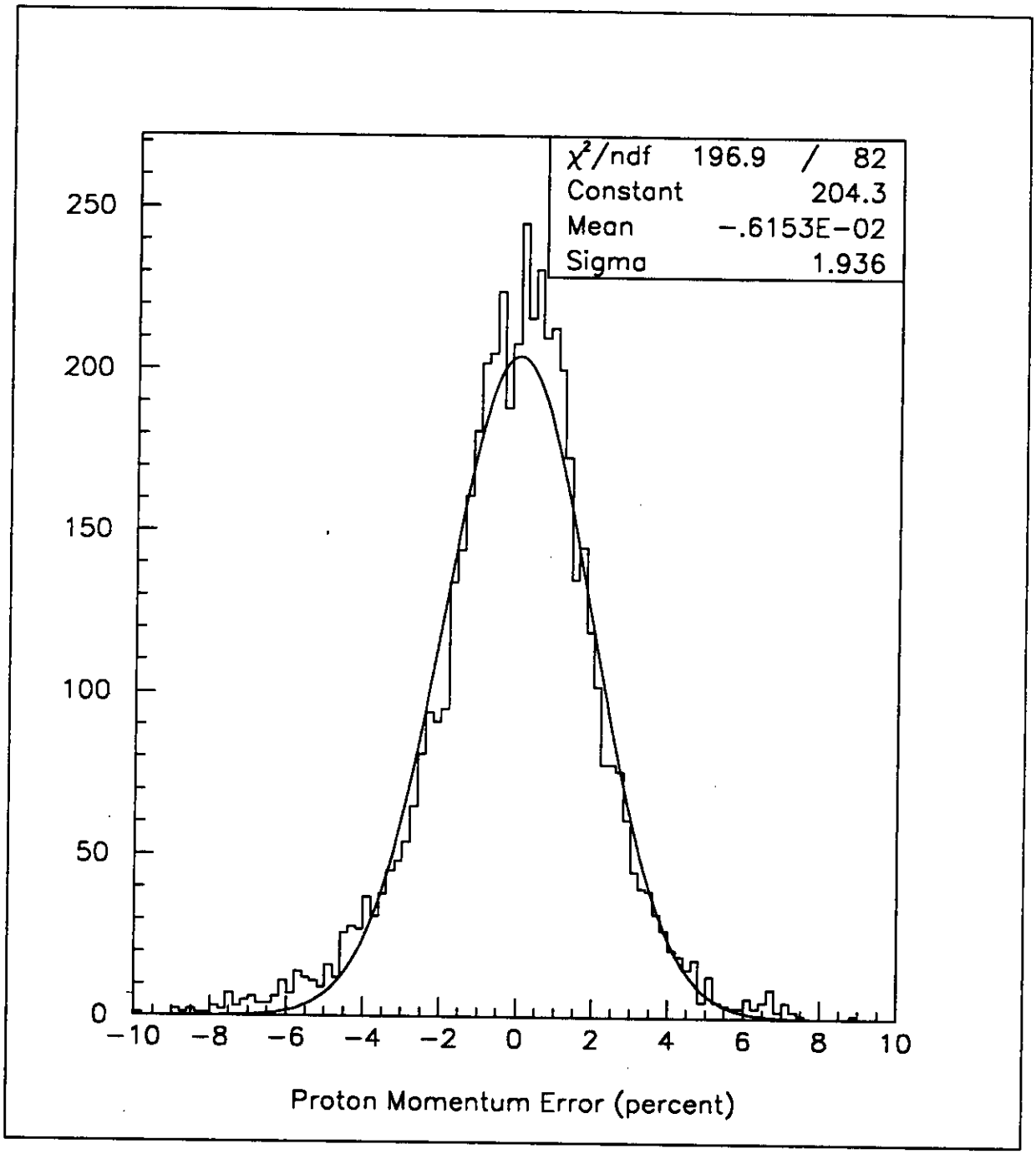


**Fig. 13. Resolution of the proton momentum in % from a SDA simulation.**

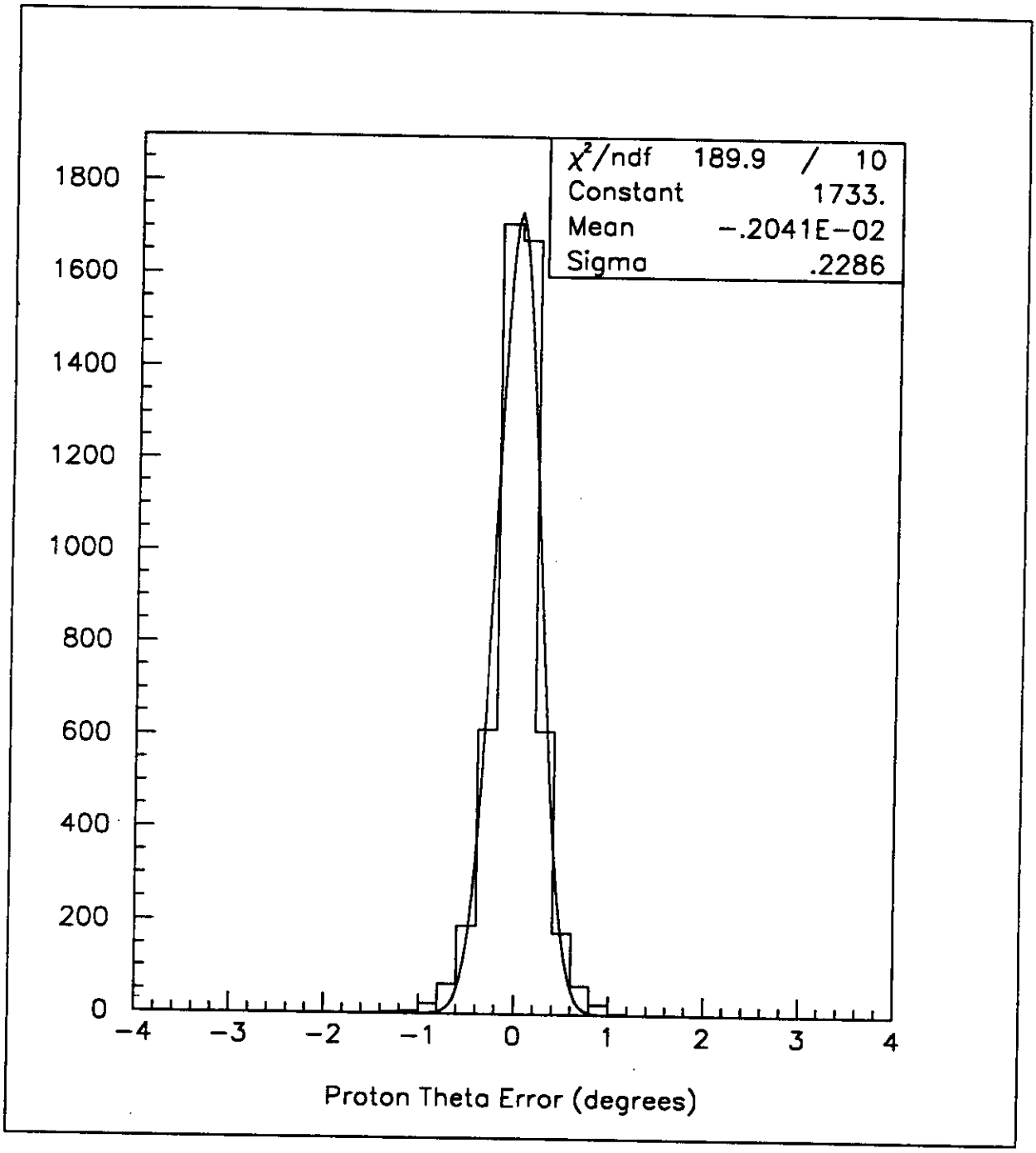


Fig. 14. Resolution of the proton angle in degrees from a SDA simulation.

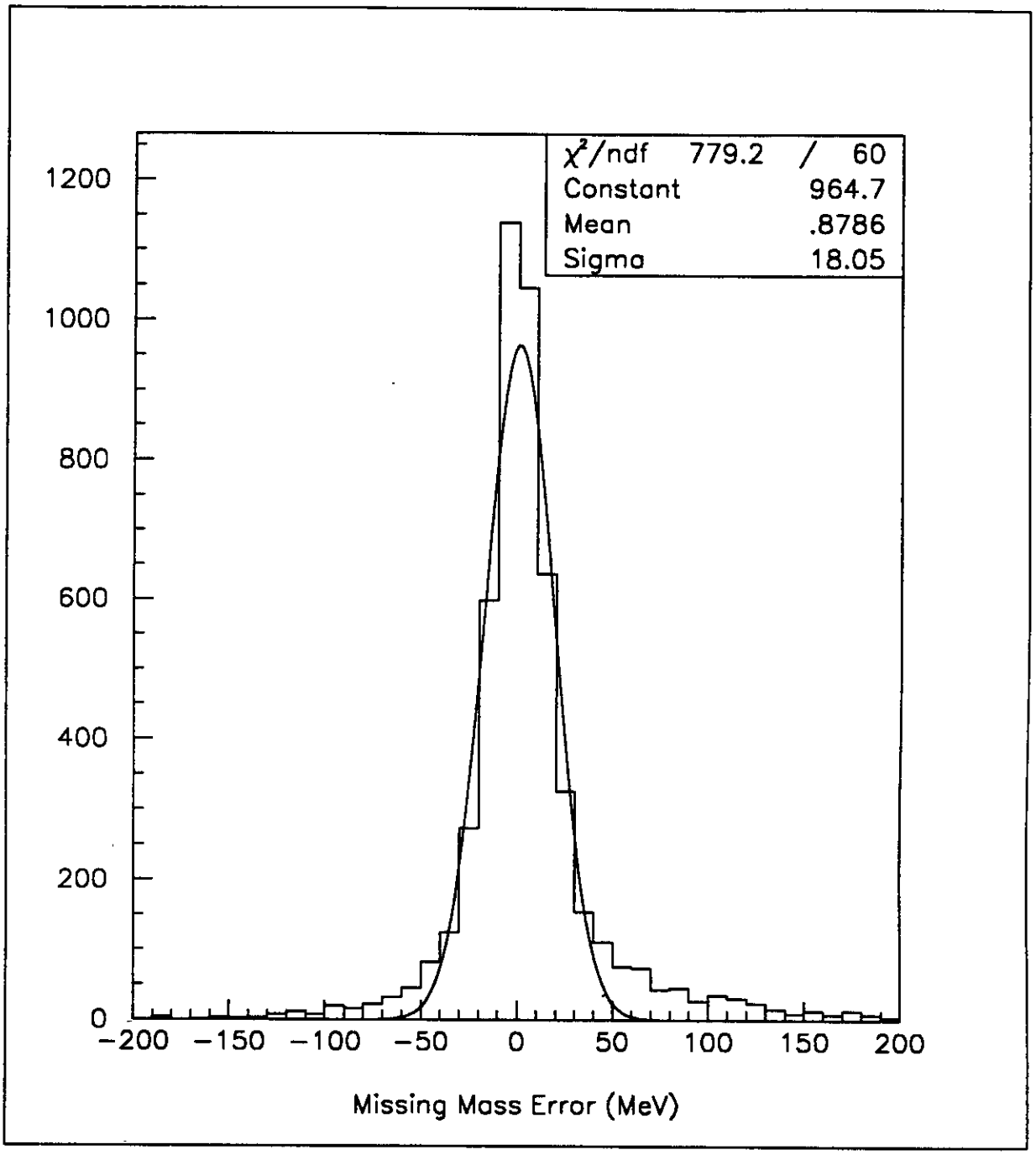


Fig. 15. Expected resolution in the missing mass $W$ of the unobserved final state of the struck neutron, from a SDA simulation.

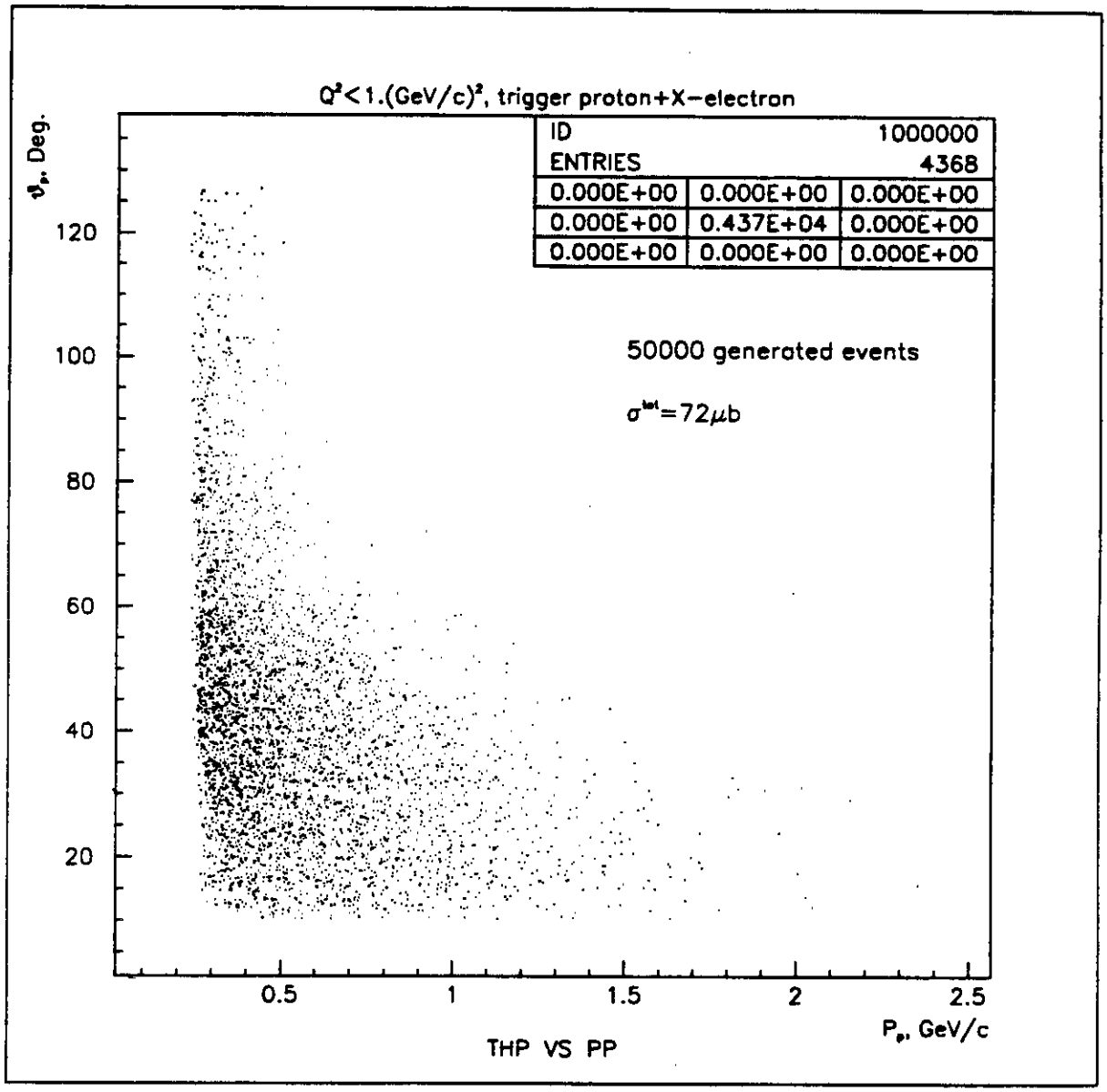


Fig. 16. Distribution in (lab) angle and momentum of single protons without detection of an electron in coincidence from a CELEG simulation.

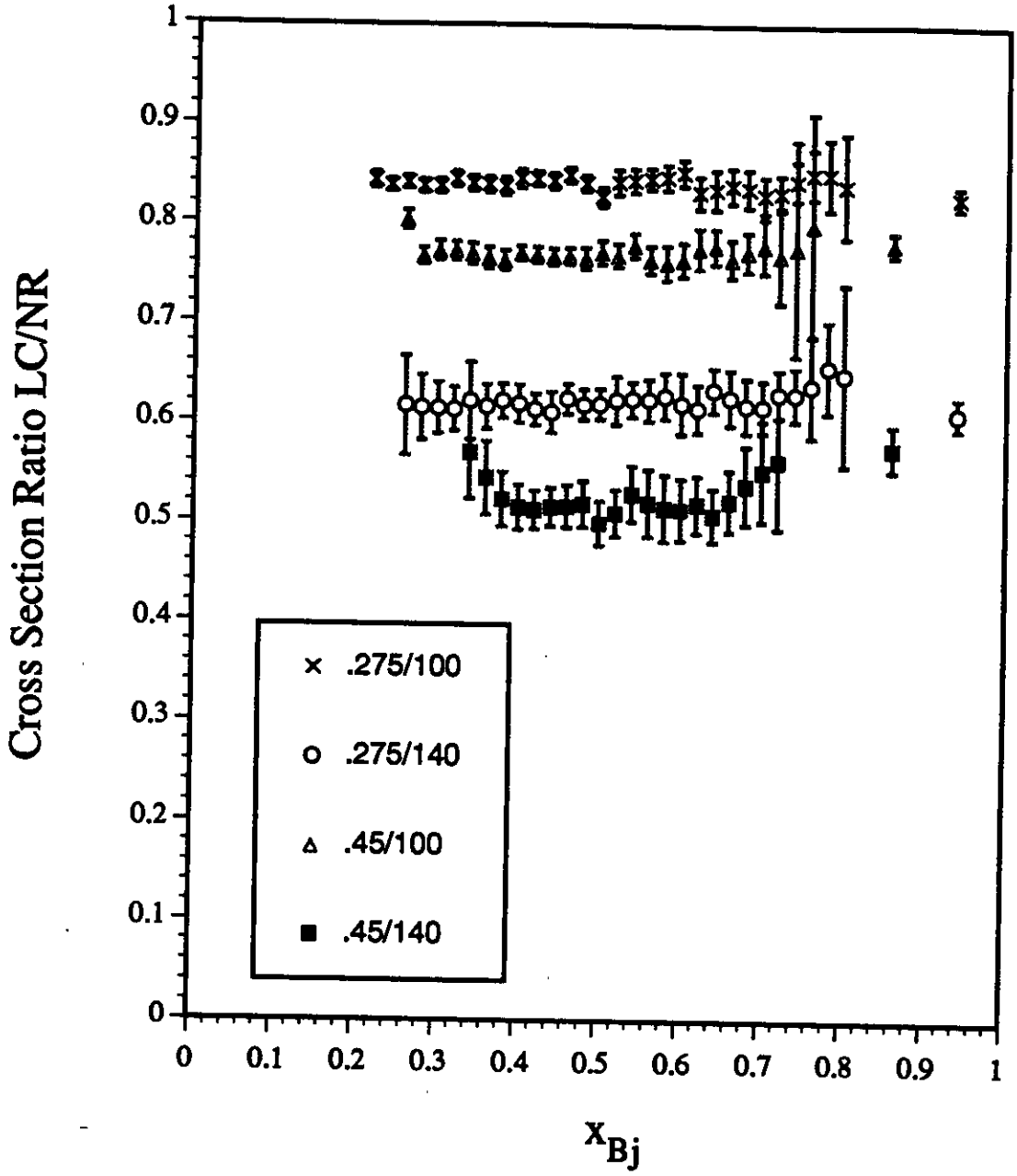


Fig. 17. Ratio of the cross section for the reaction d(e,e'p)X calculated in the light cone formalism[1] divided by the same cross section from a non-relativistic simulation, within the spectator model. The error bars indicate the expected accuracy of our data points. The square and round data points indicate the result for spectator momenta $p_s = 0.25 - 0.3$ GeV/c for the angular range $\theta_{pq} = 90° - 110°$ and $\theta_{pq} = 130° - 150°$, respectively. The triangular and diamond points are for the same angular ranges, but spectator momenta of $p_s = 0.4 - 0.5$ GeV/c. The prediction from the non-relativistic model is independent of $\theta_{pq}$.

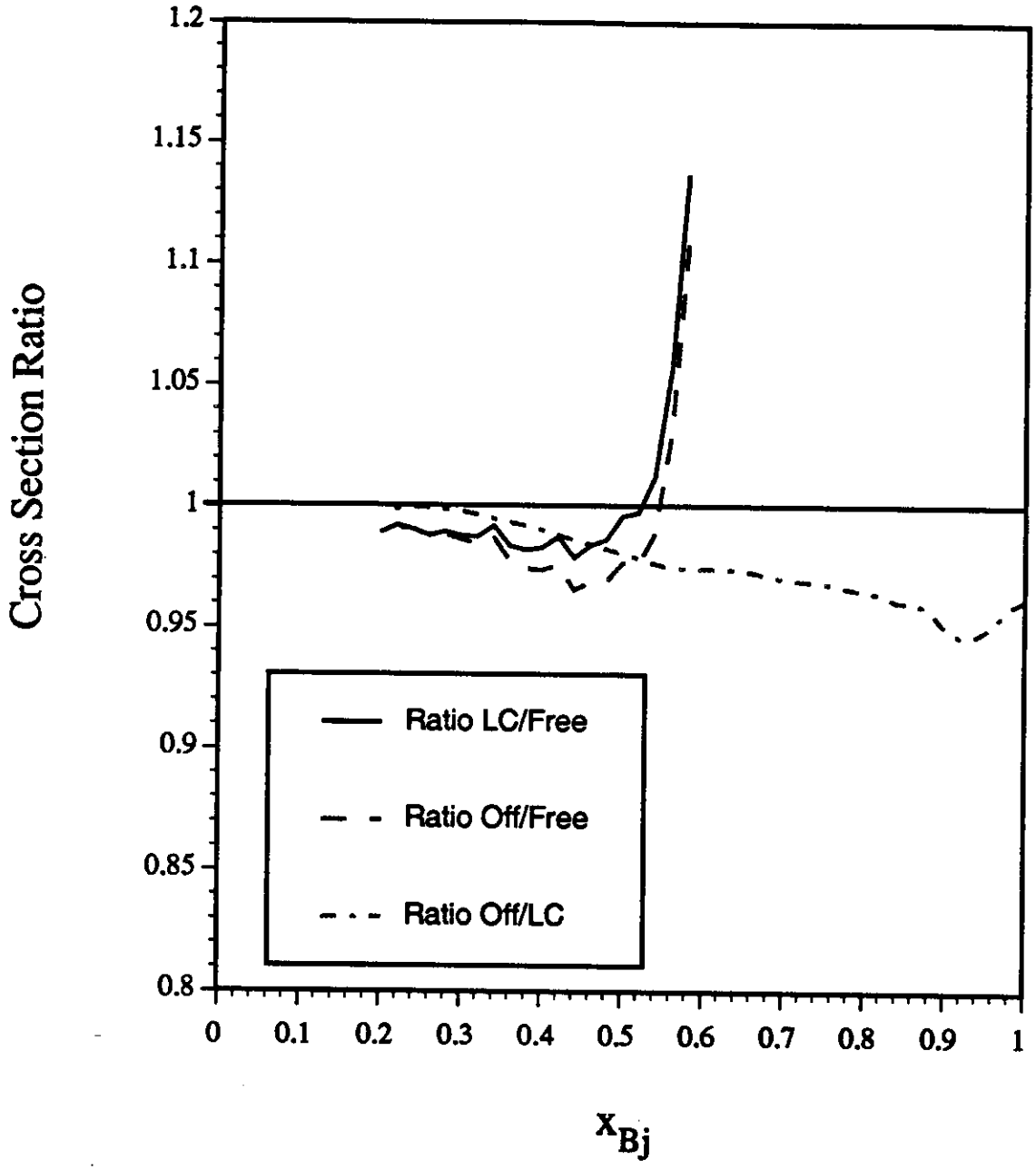


Fig. 18. Ratio of the average cross section on a bound neutron in deuterium to the free one in the light cone formalism. Shown are both the on-shell (solid line) calculation and the result for the off-shell model of Ref.[1] (dashed line). The dot-dashed line is the ratio between off-shell and on-shell calculations.

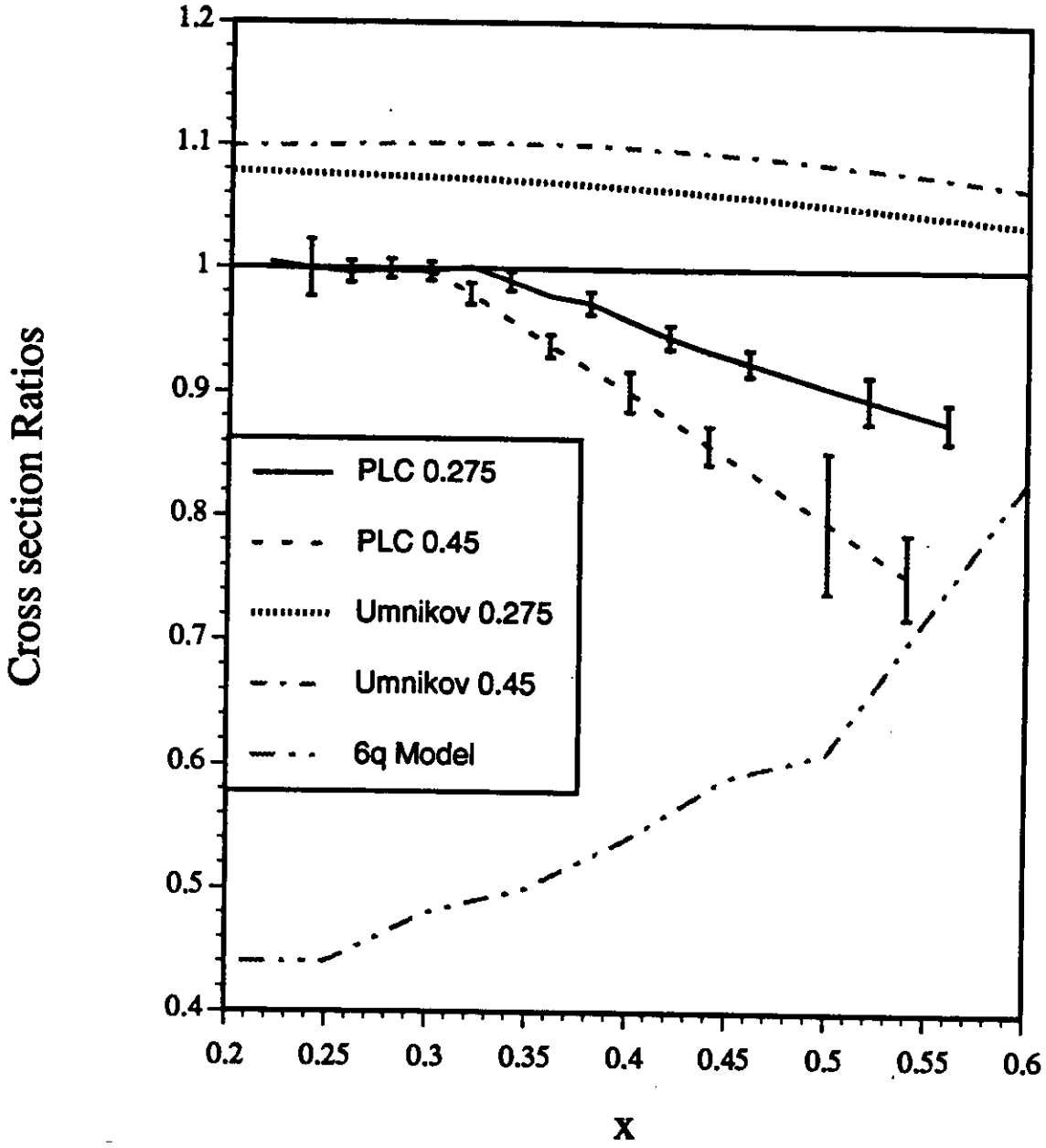


Fig. 19. Ratio between several different predictions of the cross section d(e,e'p)X in the deep inelastic region ($Q^2 = 2 \pm 0.5, W \geq 2$) and the on-shell cross section calculated in the light cone formalism (Eq. 3). The solid and dashed lines are for an off-shell calculation following the PLC suppression model of Frankfurt and Strikman[1] for two different ranges of backward proton momenta: $p_s = 0.25 - 0.3$ GeV/c and $p_s = 0.4 - 0.5$ GeV/c. The dotted and the dashed-dotted line are predictions by Umnikov et al.[14] for the same momentum ranges. The dash-double-dotted curve indicates the expectation for scattering from a 6-quark object following the model of Carlson and Lassila[6]. The error bars indicate the expected accuracy of the proposed experiment.